Title

A high-quality reference genome for the Ural Owl (*Strix uralensis*) enables investigations of cell cultures as a genomic resource for endangered species

Authors

Ioannis Chrysostomakis[1], Annika Mozer[1], Camilla Bruno Di-Nizo[1], Dominik Fischer[2], Nafiseh Sargheini[3], Laura von der Mark[1], Bruno Huettel[3], Jonas J. Astrin[1], Till Töpfer[1], *Astrid Böhne[1]

*corresponding author

Affiliations

[1]Leibniz Institute for the Analysis of Biodiversity Change, Museum Koenig Bonn, Adenauerallee 127, 53113 Bonn, Germany

[2]Zoo Wuppertal, Wuppertal, Germany

[3]Max Planck Genome-Centre Cologne, Max Planck Institute for Plant Breeding Research, Carl-von-Linne-Weg 10, 50829 Cologne, Germany

Emails

I.Chrysostomakis@leibniz-lib.de, a.mozer@leibniz-lib.de, C.DiNizo@leibniz-lib.de, fischer@zoo-wuppertal.de, nsargheini@mpipz.mpg.de, L.vonderMark@leibniz-lib.de, huettel@mpipz.mpg.de, J.Astrin@leibniz-lib.de, T.Toepfer@leibniz-lib.de, a.boehne@leibniz-lib.de

Abstract

Background

Reference genomes have a wide range of applications. Yet, we are from a complete genomic picture for the tree of life. We here contribute another piece to the puzzle by providing a high-quality reference genome for the Ural Owl (*Strix uralensis*), a species of conservation concern and efforts affected by habitat destruction and climate change.

Results

We generated a reference genome assembly for the Ural Owl based on high-fidelity (HiFi) long reads and chromosome conformation capture (Hi-C) data. It figures amongst the best avian genome assemblies currently available (BUSCO completeness of 99.94 %). The primary assembly had a size of 1.38 Gb with an N50 of 90.1 Mb, while the alternative assembly had a size of 1.3 Gb and an N50 of 17.0 Mb. We show an exceptionally high repeat content (21.07 %) that is different from those of other bird taxa with repeat extensions. We confirm a *Strix* characteristic chromosomal fusion and support the observation that bird microchromosomes have a higher density of genes, associated with a reduction in gene length due to shorter introns. An analysis of gene content provides evidence of changes in the keratin gene content of owls, which might be related to flight adaptations as well as modifications of metabolism genes. The population size history of the Ural Owl decreased over long periods of time with increases during the Eemian interglacial and stable size during the last glacial period. Ever since it is declining to its currently lowest effective population size. We also investigated cell culture of progressive passages as a tool for genetic resources. Karyotyping of passages confirmed no large variants, while a SNP analysis revealed a low presence of short variants across cell passages.

Conclusions

The established reference genome is a valuable resource for ongoing conservation efforts,

but also for (avian) comparative genomics research. Further research is needed to determine whether cell culture passages can be safely used in genomic research.

Keywords

Strix uralensis, Strigidae, karyotyping, genome sequence, genome annotation, cell culture, SNP, variant

Background

High-quality reference genomes are rapidly becoming available for many branches of the tree of life (https://www.earthbiogenome.org). These data are now increasingly used for comparative genomic studies on large evolutionary timescales trying to link phenotypes to genotypes. However, even in genomically and traditionally well-studied groups such as birds, several lineages still lack high-quality reference genome assemblies that would allow for detailed studies of genome evolution.

Typical avian karyotypes are composed of macro- and microchromosomes (but see [1,2]). Compared to macrochromosomes, which are typically between 30 and 250 mega base pairs (Mb) in size, microchromosomes have an average size of 12 Mb, although microchromosomes as small as 3.4 Mb have been observed [3,4]. Despite recent efforts to characterise avian genomes and understand their karyotype evolution, less than 10% of all known bird species have a characterized karyotype [5]. The diploid number of about half of these varies between 78 to 82 chromosomes [1]. Regarding the family Strigiformes (owls), karyotype information is available for 13 % of species [5]. Interestingly, microchromosomes encode half of the genes in birds, although they account for only about a quarter of the genome sequence [3,6]. Moreover, the mutation rate of microchromosomes is significantly higher than that of macrochromosomes [7]. Therefore, avian karyotypes, genome structure and especially the microchromosomes deserve more cytogenetic and molecular attention.

To this aim, we here provide a first high-quality reference genome for the Ural Owl (*Strix uralensis*). This species is one of the largest Eurasian owls, inhabiting the Palaearctic lowlands up to the treeline, mainly in the taiga forest belt over a large uninterrupted range from Scandinavia through Siberia to Sakhalin and the Japanese islands. It also occurs in geographically isolated, mixed and deciduous forests of southeastern and central Europe (southern Germany, Czech Republic, Austria, Slovenia and Poland; partly supported by reintroductions). So far, 11 subspecies have been described from its vast distribution based

on differences in size and colouration [8]; although not all of these have been widely accepted [9]. Furthermore, the molecular data at hand (i.e., mitochondrial and nuclear marker genes) do not support morphology-based taxonomic distinctions [10].

Ural Owls are nocturnal hunters of small mammals and birds and usually stay in their territories throughout the year [9,11]. As the Ural Owl is sedentary and nests in hollow stumps or tree holes [12,13], it is affected by ecosystem degradation [14]. Nesting sites have been reduced by intensive logging activities, agricultural use, and forestry management [8]. Direct persecution mainly drove the extinction of *S. uralensis* in Austria, southern Germany, and the Czech Republic in the last century [15–17]. Successful reintroductions have taken place in these countries (e.g. [15–17]). These central European reintroductions have restored gene flow between the remaining Alpine and European populations [10,18]. The Ural Owl will likely further be affected by climate change, potentially shifting its range to more northern regions [19] and altering breeding times [20].

Cryobanking, defined as the preservation of viable cells and tissues at ultracold temperatures, typically using liquid nitrogen, is considered paramount in preserving the genetic variability of species, especially those facing population decline as the Ural Owl, to ensure population health and persistence [21,22]. Although some instances have been reported where long-term cell culture generated genetic instability and heteroploidy [23,24], it is still unclear how frequent such a phenomenon is and at which stage of cell cultivation it occurs.

Herein, we generated a reference genome for the Ural Owl as a genomic resource to facilitate further research on this species and on Strigidae more generally. We assess the genome assembly quality and provide a first analysis of its gene content. As a species of potential conservation concern and as a proof of principle, we assessed the application of cell culture to produce sufficient DNA in terms of quantity and quality to allow genomics for species with limited biological material. We investigated mutation as a function of passage number (i.e., the transfer of cells from vessel to vessel). To this end, we obtained a cell culture from the same individual that was genome-sequenced, and cultivated the cell lines until passage 10

106 and subsequently sequenced replicates of passages 5 and 10 (Figure 1).

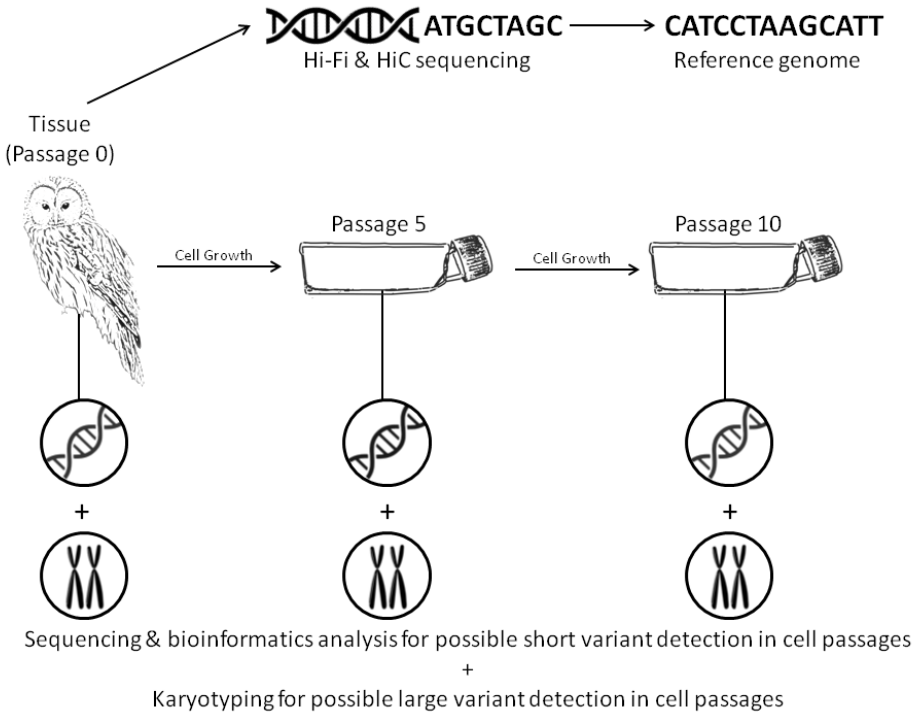

107 **Figure 1: Reference genome and cell passage variant detection workflow.** Tissue from a
108 male Ural Owl (*Strix uralensis*) is extracted and sequenced, assembled and annotated to
109 provide a reference genome. Additionally, a cell culture is established from the primary tissue.
110 From passage 0 (primary tissue), passage 5 (three independent replicates) and passage 10
111 (four independent replicates) cells are harvested for short-read sequencing and karyotyping.

Data Description

In order to provide valuable genomic resources to the scientific community studying avian ecology and phylogenomics and to investigate the potential of lab-grown cells for use in DNA sequencing, skin cells were harvested from a 10-year-old, recently deceased male Ural Owl individual. The skin samples were, originally, frozen at -80°C and later grown in an appropriate medium and used for DNA sequencing. We performed PACBIO long-read sequencing of muscle tissue, which produces high-quality, long DNA fragments. We used cultured cells for Hi-C sequencing, which allows us to estimate physical proximity of DNA molecules inside the cell to create the most complete bird genome assembly to date. Next, we grew the harvested skin cells for multiple generations to understand whether this process causes damage to chromosome structure and the accumulation of DNA mutations. In the future, this data can be used to study avian phylogenomics and diversity as well as further understand the unique traits of owls. All sequence data of this study can be accessed from INSDC under the BioProject ID PRJNA1212906. Processed data are available from Zenodo under DOI 10.5281/zenodo.14676512.

Analyses

Read quality control and estimation of genome size and heterozygosity

After quality control, filtering, and decontamination the final set of HiFi reads used was composed of 5,078,732 million reads with a total length of ~58 Gb and the Hi-C reads used were composed of 79.7 million reads with a total length of ~ 20 Gb.

Using a k-mer size of 21, genomescope was able to predict a genome size of 1,292,799,460 bp, a repeat length of 188,615,362 bp, a heterozygosity of 0.2 % (this would translate to 2 heterozygous sites per 1 kb, a commonly reported heterozygosity indicator for birds) and a read error rate of 0.14 % (Supplementary Table S1). Smudgeplot and GenomeScope both verified the diploid status of the individual. (Supplementary Figure S1; Figure 2). The genome did not reveal any large runs of homozygosity (ROH).

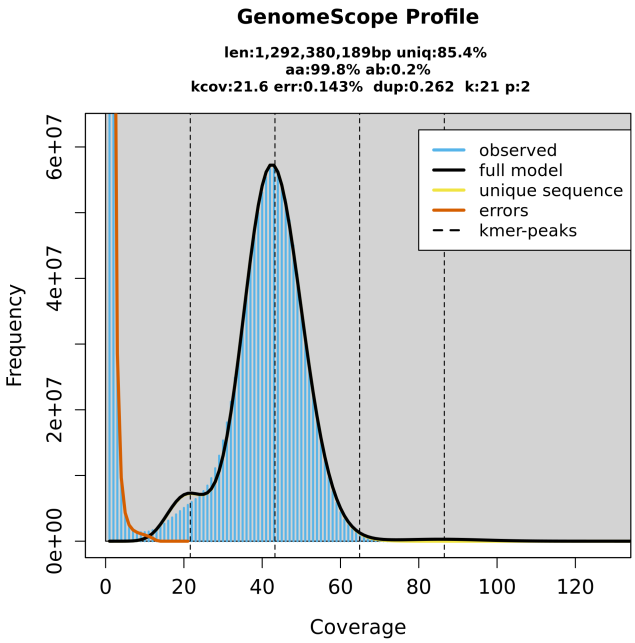

Figure 2: K-mer genome profile of *Strix uralensis* generated from PacBio HiFi reads with GenomeScope2.The y-axis shows the k-mer counts and the x-axis shows sequencing depth. The first peak corresponds to heterozygous k-mers and the second larger peak to homozygous k-mers with a coverage of ~42 x.

Reference genome

The optimal assembly was created with Hifiasm parameters “-l2 --n-weight 5 --n-perturb 50000 --f-perturb 0.5 -D 10 -N 150 -s 0.4” (Supplementary Table S1).

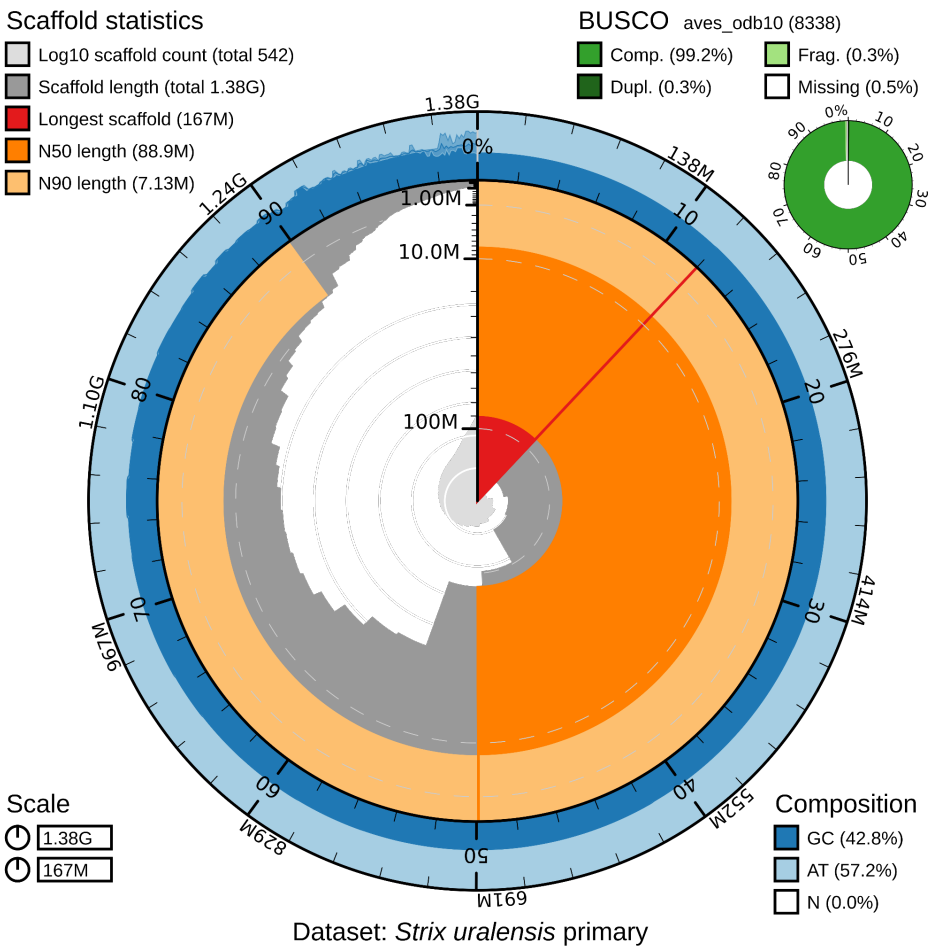

Dataset: *Strix uralensis* primary

Figure 3: Snail plot summary of assembly statistics for *Strix uralensis* primary assembly. The main plot is divided into 1,000 size-ordered bins around the circumference with each bin representing 0.1% of the 1,381,000,783 bp assembly. The distribution of sequence lengths is shown in dark grey with the plot radius scaled to the longest sequence present in the assembly (166,530,430 bp, shown in red). Orange and pale-orange arcs show the N50 and N90 sequence lengths (88,922,949 and 7,132,230 bp), respectively. The pale grey spiral shows the cumulative sequence count on a log scale with white scale lines showing successive orders of magnitude. The blue and pale-blue area around the outside of the plot shows the distribution of GC, AT and N percentages in the same bins as the inner plot. A summary of complete, fragmented, duplicated and missing BUSCO genes in the aves_odb10 set is shown in the top right.

Genome Quality Metrics

We could place 93.6 % of assembled scaffolded genome sequence data into 41 chromosomes, which is consistent with the karyotype of the species (Figure 3). We also detected no contamination as all scaffolds aligned to sequences of other avian genomes (Figure 4). Our Hi-C contact map further supported the high contiguity of the primary assembly, by showing no remaining conflicts and little to no scaffolds with strong contacts to non-repeat regions (Figure 5).

The Merqury Quality Value (QV) score, which is the proportion of the assembly sequence supported by HiFi reads, was estimated for both haplomes. We obtained a score of 64.2 (equivalent to an error probability of 3.8238e-07 %) for the primary and 57.4 (equivalent to an error probability of 1.80919e-06 %) for the alternate assembly (Supplementary Table S2). We also find a completeness score of 98.36 % for the primary and a combined 99.81 % for the two haplomes, representing the fraction of high-quality k-mers from the reads present in the assembly. This further supports the completeness and accuracy of the assembly (Supplementary Table S2).

Aligning the PacBio HiFi, and Illumina Hi-C reads to both haplomes revealed comparable coverage levels (primary: 41.78 ± 12.18, 14.18 ± 91.47-fold respectively; alternate: 34.15 ± 23.24, 12.10 ± 107.37 respectively), mapping rates (primary: 99.85 %, 99.92 % respectively; alternate: 80.52 %, 86.6 % respectively) and mapping quality scores (primary: 36.93, 28.90 respectively; alternate: 28.11, 8.2 respectively). These results further indicate that the assembly is well-phased with a minimal amount of assembly bias and errors (Supplementary Table S3).

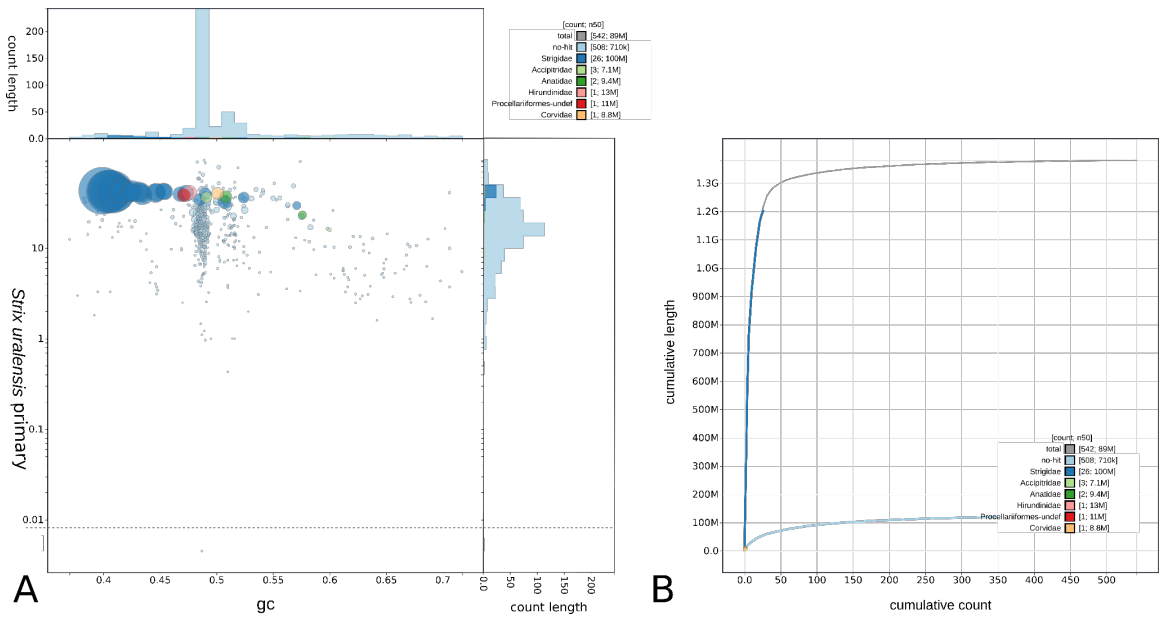

Figure 4: *Strix uralensis* primary haplome BlobToolKit GC-coverage and cumulative sequence plots. A) Blob plot of base coverage in *S. uralensis* against GC proportion for sequences in *S. uralensis* primary haplome. Sequences are coloured by phylum. Circles are sized in proportion to sequence length. Histograms show the distribution of sequence length sum along each axis. **B)** Cumulative sequence length for *S. uralensis* primary assembly. The grey line shows cumulative length for all sequences. Coloured lines show cumulative lengths of sequences assigned to each phylum using the buscogenes taxrule.

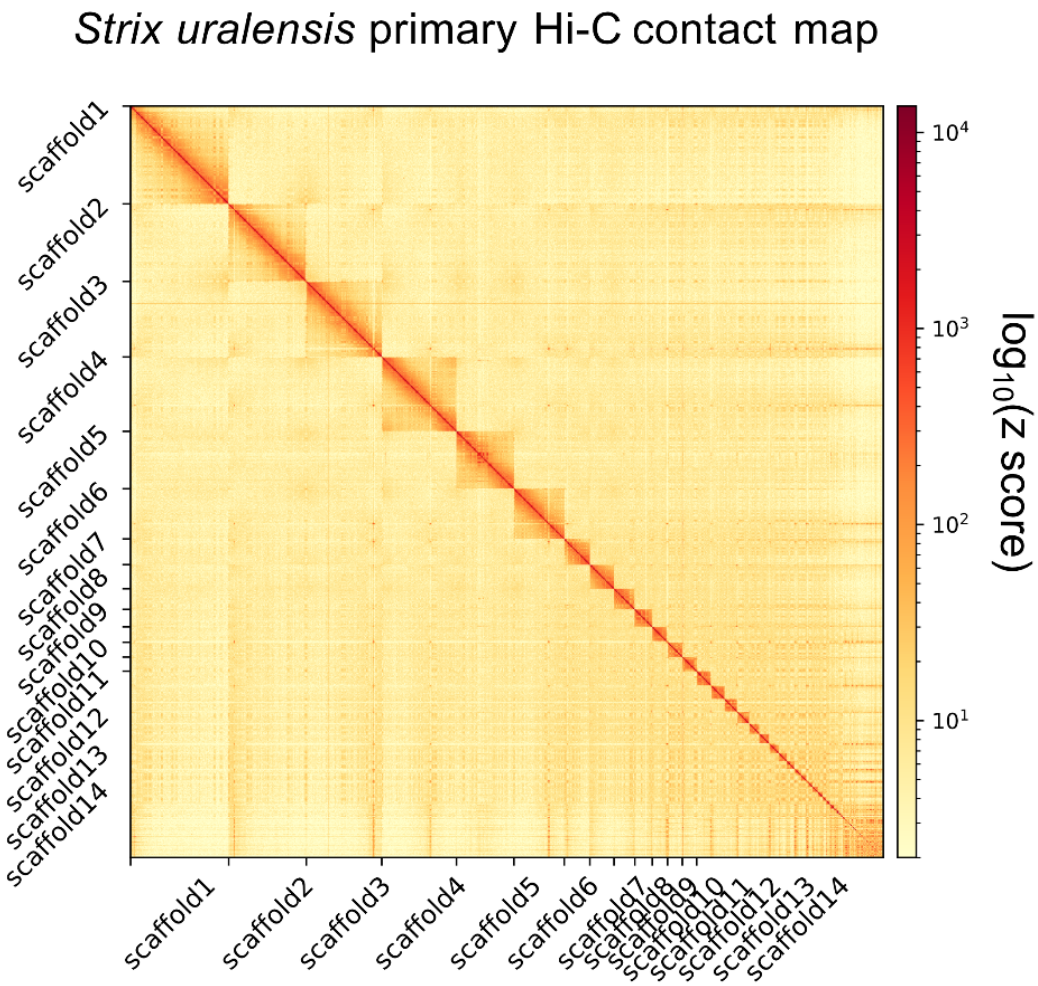

Figure 5: *Strix uralensis* primary haplome Hi-C contact map showing spatial interactions between chromosomes. Chromosomes are ordered by size from left to right and from top to bottom. The red diagonal corresponds to intra-chromosomal contacts and depicts chromosome boundaries. The frequency of contacts is shown on a logarithmic heatmap scale. Plot generated with HiCExplorer.

192 **Table 1**: Assembly statistics of the primary and alternate genome assembly of *Strix uralensis*.

Assembly statistics	**Primary**	**Alternate**
Assembly size [bp]	1,381,008,983	1,262,176,999
GC content [%]	42.77	42.81
Contigs	512	15,615
N50	90,173,155	17,018,198
L50	6	18
L90	28	8,171
Ns per 100 kb	2.94	68.29
Merqury Error (%)	3.82794e-07	1.80919e-06
Merqury QV score	64.17	57.43
Complete BUSCOs [%]	99.94	70.82

Genome Repeat and Gene Annotation

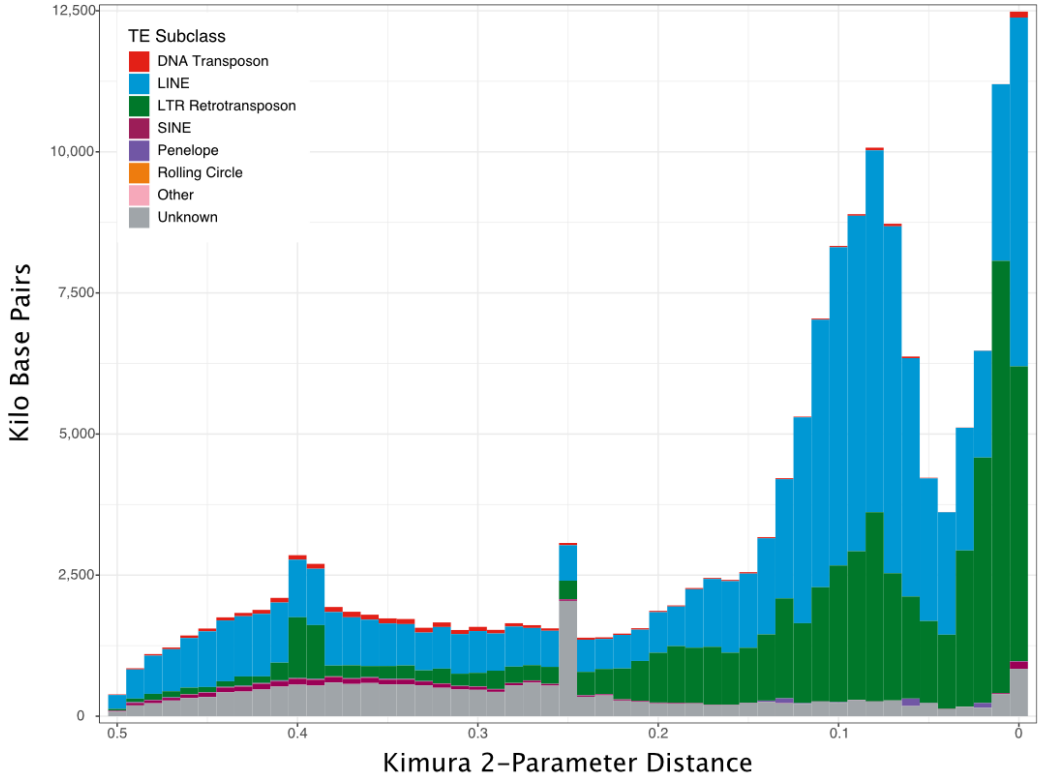

Figure 6: *Strix uralensis* primary haplome repeat landscape. The x axis shows the Kimura substitution of detected repeat categories and the y axis the number of repeats detected for each TE family in kilo base pairs. Detected subclasses are colour-coded as indicated in the inset. The genome assembly was masked using EarlGrey.

Repeat landscapes depict the clustering of transposable elements (TEs) in relation to their Kimura substitution rates, which measures the divergence of TEs from their respective consensus sequence. Lower Kimura substitution rates indicate recent transposition events, while higher rates suggest older events. From the landscape of the primary haplome (Figure 6, Supplementary Figures S2 and S3), a strong signal for a recent repeat expansion of LINEs (long interspersed nuclear elements) and an even more recent expansion of LTR (long terminal repeat) retrotransposons as well as a well-maintained large number of older repeats are visible. This might support a repeat expansion in the Ural Owl or the genus *Strix*. A third and older expansion is dominated by LINEs and unknown repeats suggesting that they are either a new or unique feature of *Strix* and a reference or consensus might not yet exist in the reference databases.

Gene annotation

For the primary haplome, we were able to annotate a total of 17,977 protein-coding genes which cover ~33.6 % of the total size of the assembly (Supplementary Table S4). We detected 182,313 exons and 164,373 introns. Compared to the Swiss-Prot and UniProt databases we were able to match 16,461 and 17,511 of our genes to annotations respectively (Supplementary Table S5).

We next investigated gene distribution along the genome. Using a 30 Mb cutoff [3,4], we identified ten macrochromosomes and 31 microchromosomes based on our assembly (Figures 5 and 7). Despite their size, microchromosomes had a higher gene density than macrochromosomes. While there are comparatively more genes on microchromosomes, these genes are shorter than those on macrochromosomes, mainly due to shorter introns (Figure 7D).

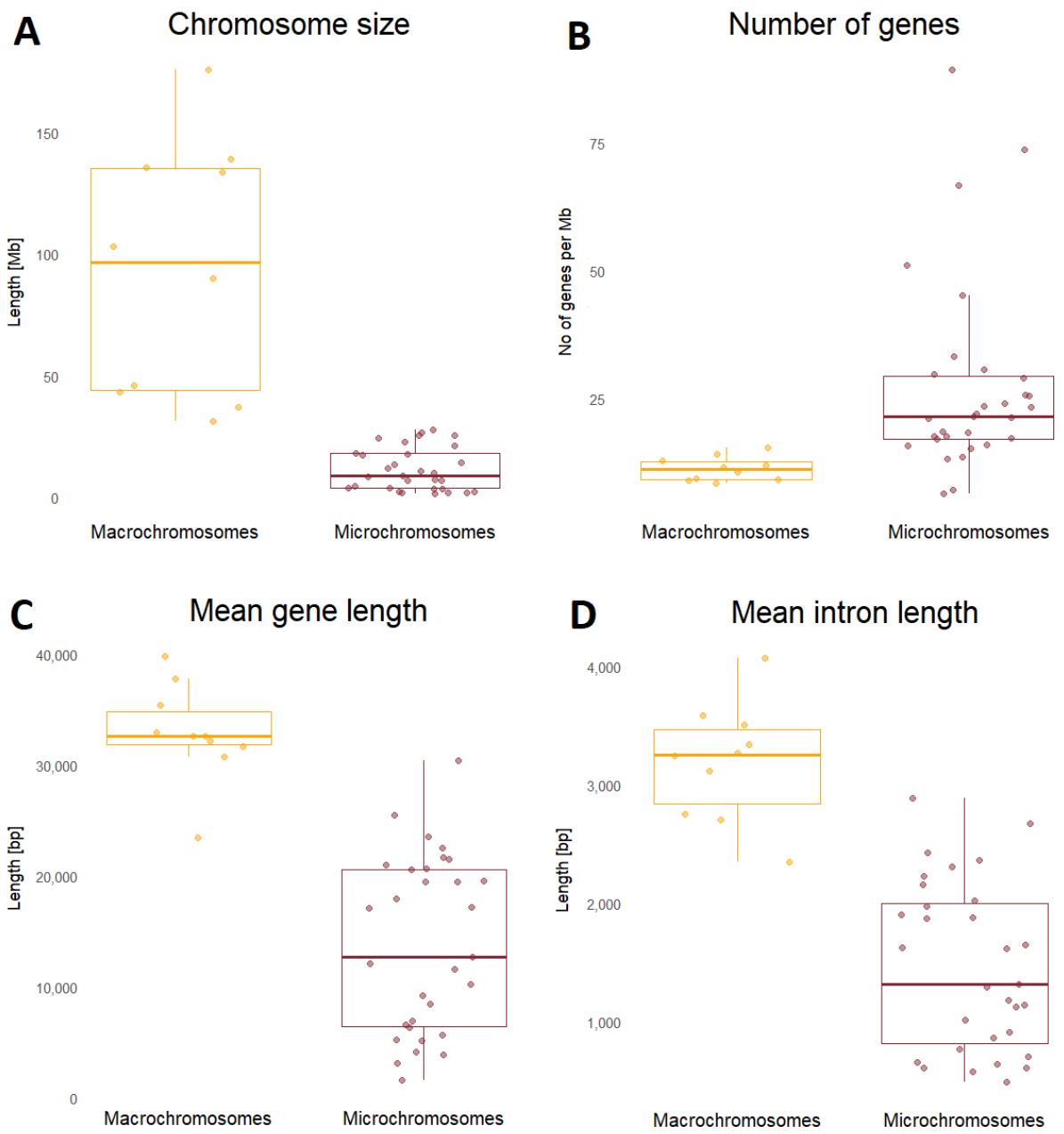

Figure 7: Gene structure of the *Strix uralensis* primary haplome. The 41 haploid chromosomes of *S. uralensis* are divided into macrochromosomes (>30 Mb; n = 10; yellow) and microchromosomes (<30 Mb; n = 31; red). **A)** Chromosome size distribution of macro- and microchromosomes, **B)** Gene density of macro- and microchromosomes. **C)** Mean gene length of macro- and microchromosomes. **D)** Mean intron length of macro- and microchromosomes. Boxplot centre lines represent the median, box limits the upper and lower quartiles and whiskers the 1.5× interquartile range. Differences were assessed using the Wilcoxon test (*** = $p \leq 0.001$).

To shed light on the genome annotation content, we compared the Ural Owl genome to other high-quality genomes of the Aves lineage, including several owl species. Gene expansion

235 (gain) and contraction (loss) among our selected species found 316 gene family gains in the
236 Ural Owl and 207 losses, 168 of which were, presumably, completely lost and, thus, have no
237 representative in the Ural Owl genome assembly (Figure 8).

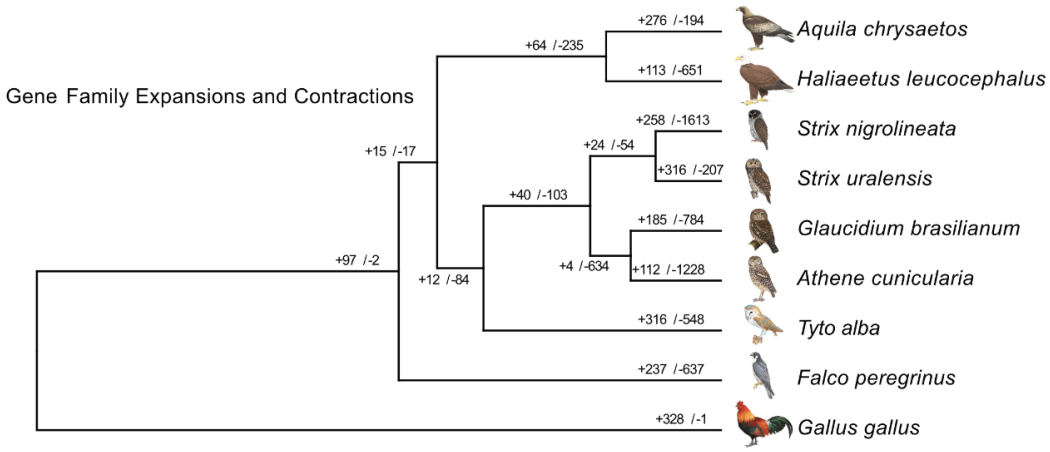

238
239 **Figure 8: Ultrametric phylogenetic tree of selected Neoaves species and *Strix uralensis*.**
240 Numbers indicate gene family expansions (+) and contractions (-). Bird drawings from
241 https://birdsoftheworld.org/.
242

243 Additionally, we found 81 gene families unique to the Ural Owl that do not have orthologs in
244 the other species (Supplementary Table S5). We further found that genomes of lower quality,
245 such as those of the Ferruginous pygmy owl, *Glaucidium brasilianum,* and the Black-and-white
246 Owl, *Strix nigrolineata*, had more gene losses, which are hence probably not biologically true
247 but represent technical limitations. A Gene Ontology (GO) term analysis of the genes unique
248 to the Ural Owl revealed many interesting gene families that due to the low quality of the Black-
249 and-white Owl genome might also be interpreted as partially representing the *Strix* genus
250 (Figure 9). Among these categories we note several GO terms relevant to characteristic traits
251 of the Ural Owl, namely its adaptation to dim-light conditions and a sedentary and predatory
252 hunting strategy. The “animal organ morphogenesis" parent GO term groups the child GO
253 terms “eye development”, “sensory organ development”, “neurogenesis” and “heart
254 development”, all of which point to adaptations of *Strix*, either to their environment or lifestyle.

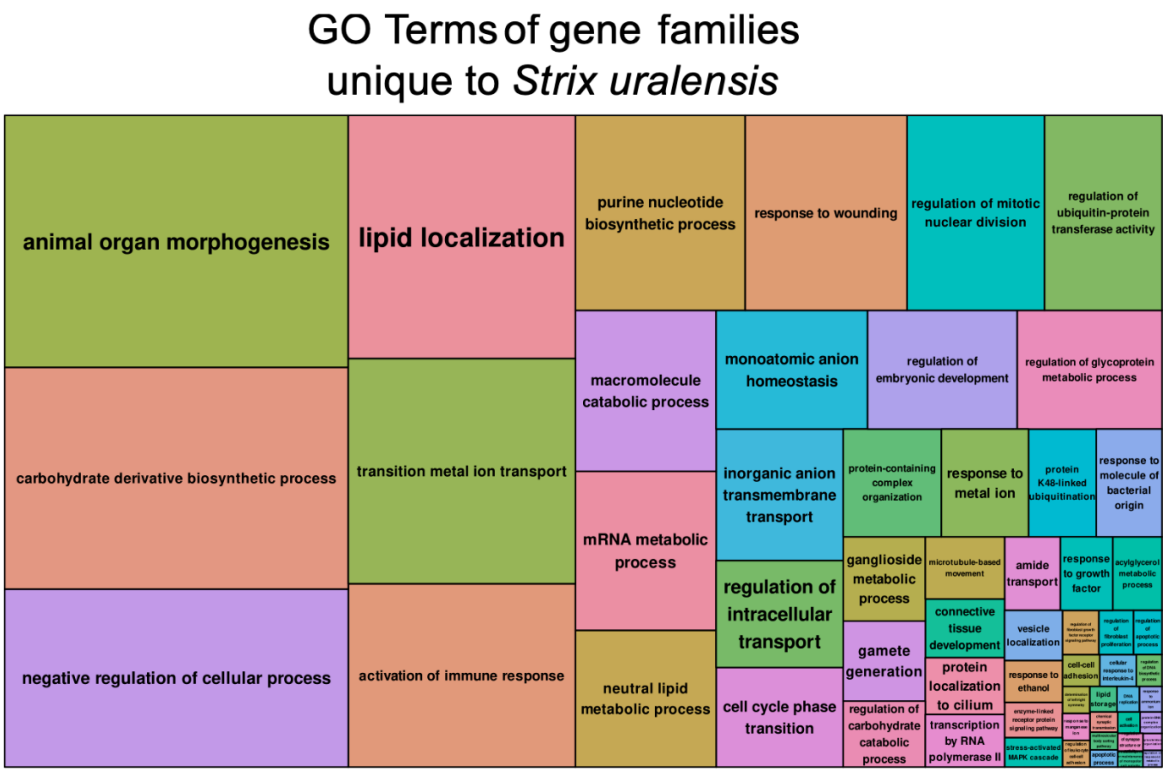

Figure 9: Treemap plot of most frequent GO term categories of gene families unique to the *Strix uralensis* primary haplome. Colour of sections is unique to each category and the size scales positively with the GO term frequency.

Next, we investigated gene gain and loss at nodes that are supported by more than one reference genome which would make them more robust and at the same time informative about clade-specific genomic changes.

We observed 15 gene family gains and 17 losses in the last common ancestor of Strigiformes and Accipitriformes (hawks, eagles, vultures, kites), both characterized by a predatory lifestyle. Overarching GO terms among the gained genes included “behavior”, metabolic, cellular and developmental processes. Notably, the child GO terms contained many terms related to general and cellular metabolism (e.g., “ATP metabolic process”, “carbohydrate derivative metabolic process”, “cellular lipid catabolic process", "cellular lipid metabolic process”). We identified three gains in keratin genes (feather and scale keratin), two related to histones/histone modification and two related to skeletal muscle functioning (BEST3, CKB).

The gene losses comprised several mitochondrial genes which we attribute to lower quality of

mitochondrial gene annotation of the used genomes since contrastingly to the ortholog based results, we could annotate 36 out of 37 mitochondrial genes in our assembly.

The other gene losses concerned uncharacterized gene families as well as a ribonucleoprotein (IMP4), the claudin gene family encoding for tight junction proteins and a DNA polymerase.

We identified 12 gene gains and 84 losses at the basis of owls. Interestingly, we again found an expansion of the keratin gene repertoire (gain of one keratin and one scale-keratin like gene). GO parental terms of gains pointed again to metabolic changes but also those associated with the immune system. The gains contained also an olfactory receptor. The much more numerous losses were associated even at the higher level with many different GO categories again often related to metabolism (e.g., “regulation of amide metabolic process”, “pyridine−containing compound metabolic process”).

Chromosome Scale Syntenies

Synteny with the chromosome-level assemblies of *Strix aluco* and *Bubo scandiacus* confirmed the male sex of the sequenced Ural Owl genome by identifying its Z chromosome. It is the fifth largest chromosome in the Ural Owl assembly (chromosome 5). The synteny between the two *Strix* genomes shows no major syntenic differences (Figure 10). This is also mostly true in the comparison to the Snowy Owl with the exception of the Z chromosome, which shows some internal rearrangements compared to the two *Strix* species. Whether this is caused by assembly quality and accuracy remains to be investigated. Additionally, we detect a possible chromosome fusion of chromosomes 5 and 6 of the Snowy Owl into chromosome 4 of the two *Strix* assemblies. This is supported by previous cytogenetic analyses [25].

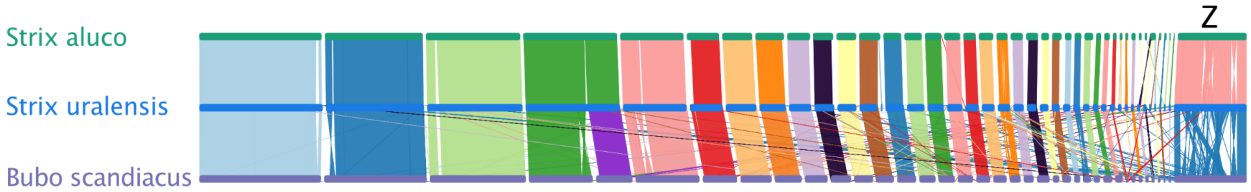

Figure 10: Chromosome scale synteny analysis. Synteny of chromosomes of *S. aluco* (top) and *B. scandiacus* (bottom) compared to the newly sequenced *S. uralensis* (middle). Syntenic regions amongst the species are indicated with a unique colour. Plot made with NGenomeSynt. Only scaffolds that mapped to the *S. uralensis* primary chromosomes were included. Assignment of sex chromosomes is based on the *S. aluco* genome annotation.

Demographic history

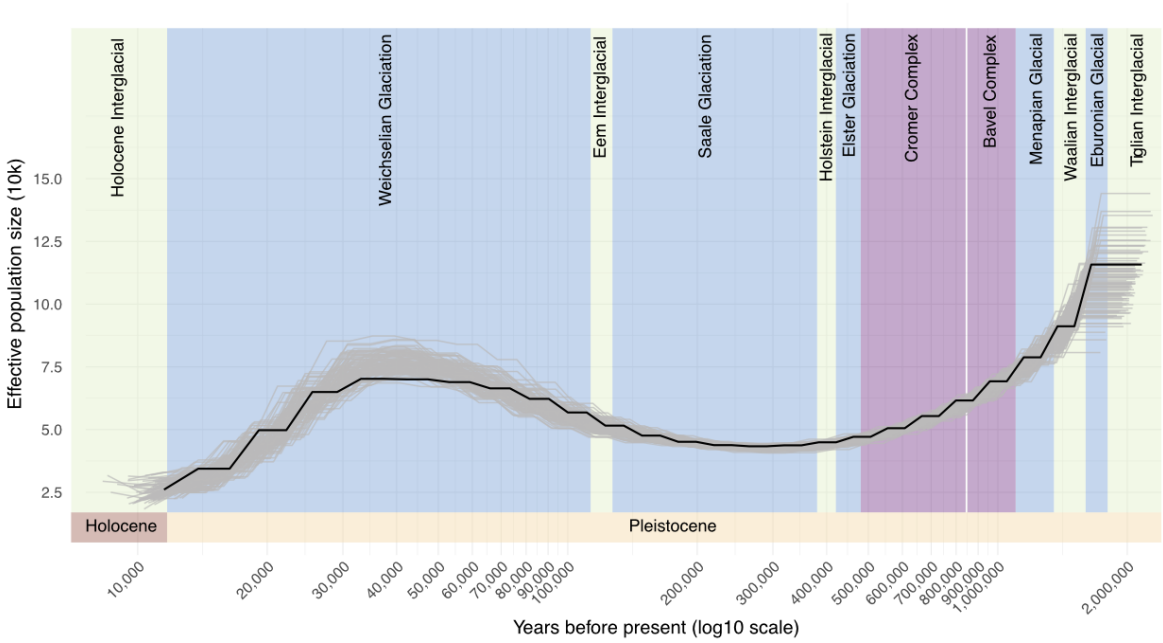

Figure 11. Inferred demographic history of *Strix uralensis.* The plot shows a Pairwise Sequentially Markovian Coalescent (PSMC) analysis based on the primary genome assembly. The x-axis shows years before present (ya) on a logarithmic scale and the y-axis shows the estimated effective population size. Bootstrap results are shown in light grey.

The demographic history of the Ural Owl derived from our genome assembly appears to have a complex relationship to glacial and interglacial periods. The effective population was predicted to have decreased until around the Holstein interglacial period (3.74 × 10^5 – 4.24 × 10^5 ya) where its population size stabilized but remained low during the Saalian glacial

period (4-1.3 × 10^5 ya) and began to increase as the Eemian interglacial period (1.3-1.15 × 10^5 ya) began to emerge. It continued to increase and reached a plateau during the last glacial period (Weichselian glaciation, 1.15-0.117 × 10^5 ya). Before the end of the last glacial period, at around 0.3 ×10^5 ya, the Ural Owl population began to decrease until it reached the current lowest effective population size (Figure 11).

Variation analysis over progressive cell passages

Karyotype confirms chromosome numbers and reveals no large variants caused by passaging

Chromosomal analyses detected 2n = 82 in both passages 5 and 10, corroborating the diploid chromosome number described for the Ural Owl previously (subspecies *S. uralensis uralensis* and *S. u. japonica*, [26]). No large-scale chromosomal rearrangements were observed between both passages (Figure 12).

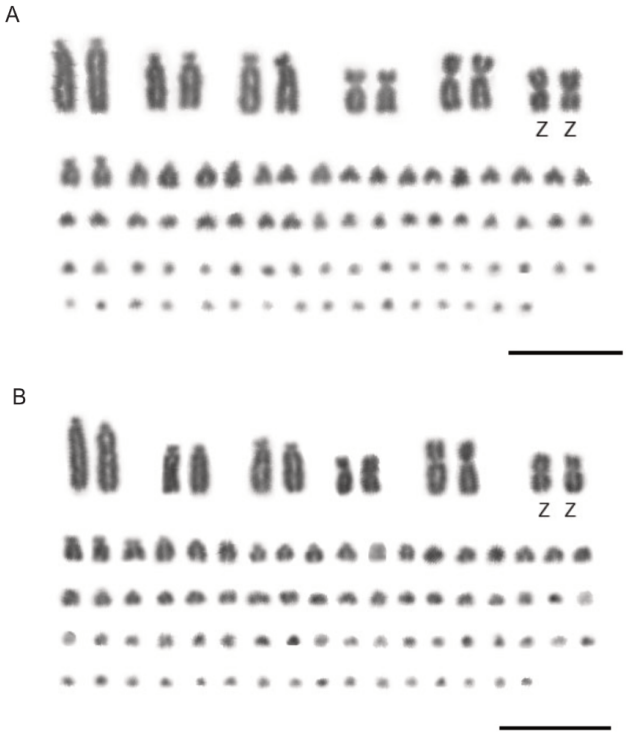

Figure 12: Karyotype analysis. Karyotype of *S. uralensis* male with 2n = 82 after passage 5 (a) and passage 10 (b). Bar = 10 µm.

Short-read variants

After quality filtering, we identified 885,159 variant sites (in the following referred to as SNPs) (Figure 13). Out of these, the vast majority (i.e., 670,463 SNPs) were fixed variant sites across all samples and hence mostly represented heterozygous sites of the individual which are represented with just one of the two alleles in the reference genome or sites that had a wrong allele in the reference assembly.

The remaining 214,696 SNPs varied across samples, indicative of potential mutations, and were analysed in the following.

A comparison of all SNPs across all samples revealed that variant amount and type differed. The biggest differences resulted from SNPs called from the HiFi data as well as the passages 5.1 and 10.1 which appear to have more SNPs than the other passages. The majority of these are heterozygous first-alternate sites (Figure 13, Table 2) and we suspect for many of those that they are false heterozygous calls rather than true mutations. To investigate this pattern further, we inspected genotype quality and depth focusing on sites with a genotype in a sample not found in any other sample (i.e., private sites) compared to the same metrics at all other sites of that individual (i.e., common variants and conserved heterozygous sites). This analysis revealed that all passages had similar median depth per variant site (DP ~26.78 ± 6.55) and genotype quality (GQ ~99), suggesting rather consistent data quality across samples (Table 2). It further showed that median depth and quality of private SNPs consistently had a significantly lower depth and quality than the average non-private site, suggesting that these alleles are to some extent wrongly called (Figure 14). To account for patterns potentially driven by sequencing technology, we also assessed in each replicate at how many positions it differed compared to passage 0. This revealed the same pattern of an increase of SNPs in samples passage 5.1 and 10.1

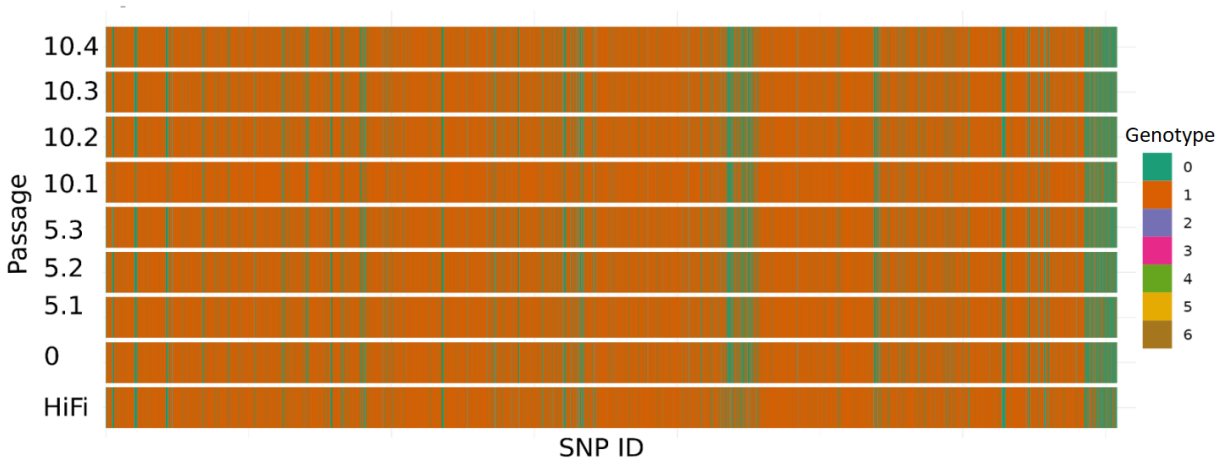

Figure 13: Variant calls of each passage. SNPs are ordered by genome position as derived from the variant filed, colour indicates allele as illustrated in the inset and referring to "0|0" = 0, "0|1" = 1, "1|0" = 1, "1|1" = 2, "0|2" = 3, "2|0" = 3, "1|2" = 4, "2|1" = 4, "2|2" = 5, "0|3" = 6, "3|0" = 6.

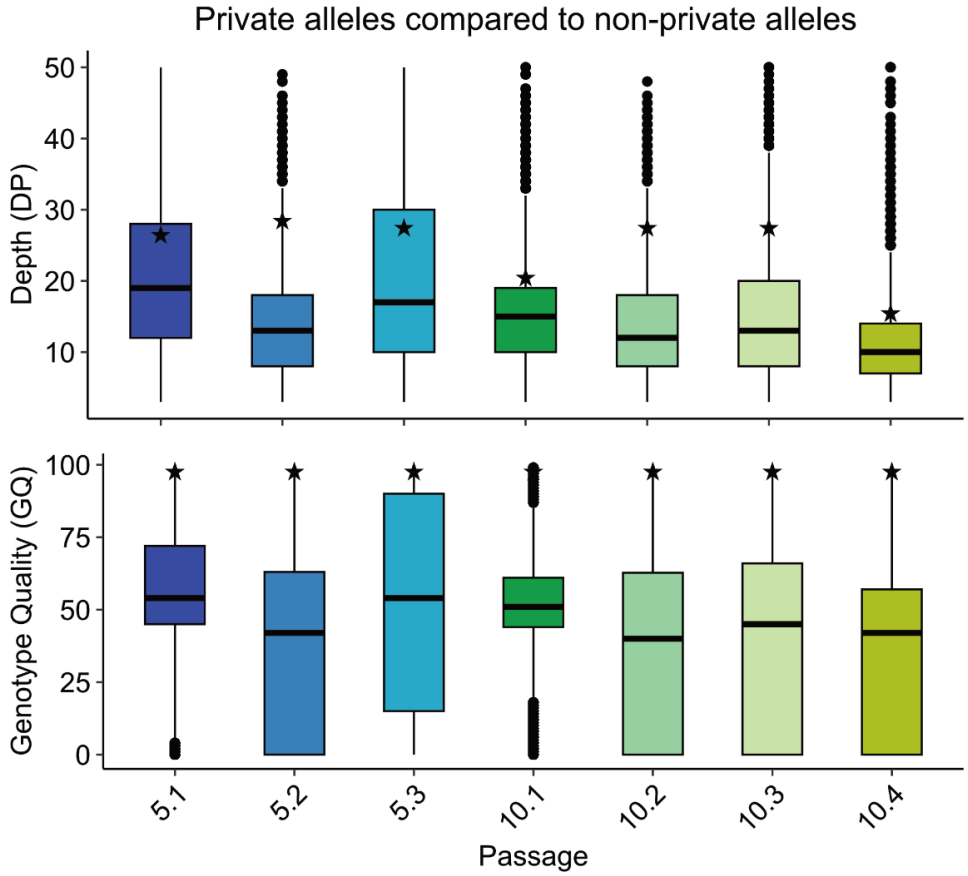

Figure 14: Quality assessment of private sites. Median depth (top) and median genotype quality (bottom) of private SNPs in each section compared to non-private SNPs (star).

357 **Table 2**: SNP statistics over progressive cell culture passages.

Sample	Median depth of variant sites	Median GQ of variant sites	SNPs other than shared heterozygous sites/private to individual	SNPs other than shared heterozygous sites as a percentage of the total genome size [%]	SNPs that are 0/1	SNPs that are not 0/1 nor 1/1	SNPs other than fixed heterozygous sites [%]	SNPs different from passage 0	SNPs different from passage 0 [%]
HiFi Reads	39	99	78,983/35,645	0.0057	77,682	1,265	0.14	-	-
Passage 0	27	99	57,929/8,212	0.0042	56,232	816	0.922	-	-
Passage 5.1	27	99	78,193/23,889	0.0057	76,709	716	0.809	58,620	6.62
Passage 5.2	29	99	55,225/3,280	0.0040	54,037	615	0.695	38,765	4.38
Passage 5.3	28	99	57,664/5,581	0.0042	56,267	781	0.882	41,301	4.67
Passage 10.1	20	99	103,086/63,058	0.0075	101,450	25	0.028	96,768	10.93
Passage 10.2	28	99	54,404/3,410	0.0039	53,373	420	0.475	38,921	4.40
Passage 10.3	28	99	55,976/3,758	0.0041	54,679	642	0.725	39,843	4.50
Passage 10.4	15	99	54,215/15,521	0.0039	52,153	750	0.847	50,033	5.65

358

Discussion

Reference genomes are accumulating across the tree of life and here birds have seen special attention fuelled by initiatives such as B10K (https://b10k.com/). Still, many of these genomes remain incomplete in terms of chromosomal-scale assembly type as well as gene annotation comprehensiveness. Genome assembly quality can impact phylogenomic inferences, analyses of gene prediction, gene family expansion and contraction, and most importantly structural evolution. In an effort to allow such analyses for the vastly understudied bird order Strigiformes, we here present a reference genome for the Ural Owl, that is among the best bird genome assemblies currently, reflected by assessments of sequence and gene completeness. We could place most of the genome into chromosomal-scale scaffolds, which are in line with the species karyotype, that we also confirm by cytogenetics. We further identified the supposedly *Strix*-specific chromosomal fusion which distinguishes it from the genus *Bubo* [2]. A first analysis of the Ural Owl genome content indicates an important increase in repetitive sequences compared to most other non-owl bird genomes. Birds on average have rather compact genomes compared to other vertebrate lineages (average ~1.1 Gb [27]), mostly owing to a low content of repetitive elements (10-15 %). Until now, owls were seemingly no exception to this with an average genome size of 1.2 Gb and a repeat content of ~8,6 % [27]. Still, cytogenetic studies already suggested differently and hint at owls being rather an exception in the avian lineage with large scale variations in karyotypes. For example, the barn owls have no distinct macro- and micro-chromosomes whereas the true owls do, suggesting chromosome fusion and fission in owls [2]. Interestingly, the recently published genome (1.6 Gb) of the Snowy Owl further extends this suspicion by demonstrating that it has one of the highest reported repeat contents for birds (28.34 %), mainly composed of centromeric satellite DNA [28]. Our assembly's total repeat content, at 21.07 % (1.5 % of which is unidentified), follows this pattern. While both owl genomes' repeat expansions are largely driven by retrotransposons, the Snowy Owl had a stronger increase of LTRs compared to LINEs than the Ural Owl. Nevertheless, LTR retrotransposons are the largest repeat class

386 also in the Ural Owl, and, especially the youngest repeat expansion is also driven by LTRs
387 suggesting this pattern to be more broadly present in true owls. In the Snowy Owl, the repeats
388 are suspected to have driven the evolution of novel centromeres. Accordingly, cytogenetic
389 analyses already identified large centromeric satellite blocks shared among and unique to true
390 owls [25]. Other bird lineages with increased repeat content are woodpeckers and the
391 Common Scimitarbill (*Rhinopomastus cyanomelas*) [27]. The cause and consequences of the
392 repeat extensions in the genera *Strix* and *Bubo* remain unclear at this point, which is also true
393 for the woodpecker [29].

394 Avian genomes are smaller than those of most vertebrates [30]. Microchromosomes have
395 been conserved for over 400 million years of vertebrate evolution. In birds, microchromosomes
396 possibly originate from chromosome fission. At the same time, recombination of
397 microchromosomes is enhanced, giving rise to two types of chromosomes,
398 macrochromosomes and microchromosomes, with different properties [3]. The number of
399 microchromosomes identified in *S. uralensis* (n = 31) is consistent with the average number
400 of microchromosomes reported by Tegelström and Ryttman [31] from karyotypes of over 230
401 bird species. However, there is no established rule for distinguishing between
402 macrochromosomes and microchromosomes (e.g. [32]). We here confirm that in birds,
403 microchromosomes have a higher gene density than macrochromosomes (e.g. [3,32–34]).
404 We could further show that the higher density of genes on microchromosomes is associated
405 with a reduction of gene length, which in turn is due to correspondingly shorter introns. A
406 similar pattern has been reported in chickens, where the size of the chromosome correlates
407 with the length of the genes it harbours [35]. Thus, in true owls, microchromosomes hold up
408 the crucial role they supposedly have played throughout vertebrate evolution [36].

409 Our assembly seems to be particularly well-suited for an analysis of gene content due to a
410 high completeness of gene annotation. However, due to vastly varying assembly qualities, the
411 correctness of our gene family expansion analysis should be taken with a grain of caution.
412 Still, this preliminary analysis suggests that in the future we will be able to connect changes in

413 gene content to adaptations of owls. This is supported by Ural Owl specific gene gains in the
414 GO-term derived function of e.g. “eye development”, “sensory organ development” and
415 “neurogenesis”, which could be linked to adaptations required for a nocturnal, predatory
416 lifestyle [37].

417 We also offer candidate genes for further investigation that characterize predatory lifestyle,
418 i.e., genes gained in the common ancestor of Strigiformes and Accipitriformes that acquired
419 this lifestyle. We especially observed gains of genes with a metabolic function which could
420 relate to the change in diet in the ancestor of these two bird orders. We also found gains of
421 keratin genes. Feathers are epidermal appendages. Vertebrate skin appendages consist of
422 two fibrous proteins, alpha and beta keratins. Interestingly, β-keratins are exclusively found in
423 reptiles and birds. Both keratin gene families show expansions in different lineages. The Barn
424 Owl had the lowest number (6) of β-keratins in a study comparing 48 bird (draft) genomes.
425 The zebra finch in comparison had 149 genes [38]. This comparison further showed that the
426 proportion of claw β-keratins and keratinocyte β-keratins is higher in predatory birds. We
427 support the latter finding with the detection of three gains of feather and scale keratins in the
428 common ancestor of Accipitriformes and Strigiformes and two further gains in the ancestor of
429 all owls. These keratin genes are candidates that could underlie morphological adaptations of
430 feathers in predatory birds in general but also more specifically in the mostly nocturnally
431 hunting owls. Their silent flight is made possible by physical characteristic fringes of the
432 feathers on the leading edge of the wings [39]. The genomic basis of this adaptation remains
433 to be identified.

434 The Ural Owl is protected under the CITES convention Annex II and the Bern Convention on
435 the Conservation of European Wildlife and Natural Habitats. While globally not yet under
436 concern, the species went extinct in Germany and other parts of Europe due to habitat
437 destruction but also direct persecution. It has subsequently been reintroduced, however due
438 to low availability of breeding couples, individuals of various origins were used for these
439 actions [16]. Breeding efforts for the species are currently undertaken by several zoos and

440 raptor centres. An analysis of marker genes neither supported morphological subspecies nor
441 did it reveal a phylogeographic population structure for the Ural Owl. Yet, it revealed genetic
442 clusters that could be informative for supportive breeding programs [10]. The here generated
443 reference genome will facilitate future genomic studies in this direction of *S. uralensis*.

444 With an estimated genome wide heterozygosity of 0.2 % (2 het/kb), the here sequenced
445 individual shows a higher level of heterozygosity than genomes of endangered bird species
446 (red list status accessed March 2025, /www.iucnredlist.org/) such as the white-eared night
447 heron (*Gorsachius magnificus*, Endangered, 0.49 het/kb) [40], Andean condor (*Vultur*
448 *gryphus*; Vulnerable, 0.75 het/kb) and California condor (*Gymnogyps californianus*; Critically
449 Endangered, 1.34 het/kb) [41], and Crested ibis (*Nipponia nippon*, Endangered, 0.043 het/kb)
450 [42]. A similar heterozygosity level as the one we estimated for the Ural Owl was detected in
451 e.g., Wild Turkey (0.24 %) and Mallard (0.26 %) [43]. It is somewhat lower than levels reported
452 for other Strigiformes such as little owl (*Athene noctua*; 0.593) [44], Tawny Owl (*S. aluco*, 0.57
453 to 0.70) [45] and Barn Owl (*Tyto alba*, 0.59 to 0.71) [46] yet twice as high than in the Burrowing
454 Owl (*Athene cunicularia*; 0.1%) [47].

455 Overall, species with a threat of going extinct show reduced levels of heterozygosity compared
456 to non-threatened related taxa [48]. In bird species, related taxa of the same order with and
457 without risk of extinction, differed quite drastically in genome-wide heterozygosity [42]. These
458 differences likely result in lower evolutionary potential, reduced reproductive fitness and may
459 contribute to species extinction [48]. Thus, maintaining wild population genetic diversity is an
460 important target of the Convention on Biological Diversity (CBD). It remains, however, to be
461 assessed at which level heterozygosity reduction causes an issue for a particular species. By
462 generating genomic data for the Ural Owl we contribute to the required knowledge for genetic
463 monitoring of biodiversity.

464 Further, our reference genome already sheds light on the demographic history of the species,
465 indicating both population contractions and expansions, apparently related to ecological
466 effects of the glacial-interglacial cycle. In particular, the pattern over the last 120,000 years

467 not only demonstrates the Ural Owl's tolerance to lower temperatures, but more importantly
468 reflects its flexible habitat choice of semi-open woodlands with a mixed composition of
469 broadleaf and coniferous species [8]. From the Eemian interglacial through the Weichselian
470 glaciation, climatic changes caused fluctuations in ice sheet extent and associated changes
471 in vegetation composition, including a gradual and/or repeated reduction in forest cover
472 leading to a treeless shrubby or grassy tundra from the mid-Weichselian (e.g., [49–51]). While
473 the open or semi-open structure of the woodland habitats favoured the Ural Owl's preference
474 for breeding and hunting grounds [8] until the mid-Weichselian, the expanding tundra
475 substantially reduced suitable habitats, leading to a marked decrease in effective population
476 size.

477 In the light of species preservation, protection and restoration, *ex situ* efforts are gaining more
478 attention. Cell culturing is a valuable and widely used technique, spanning applications from
479 basic science to biotechnology research [23]. However, there is no consensus regarding the
480 number of passages considered "safe" before cells experience metabolic changes, DNA
481 damage, and chromosomal instability. What is deemed "high passage" for one cell culture
482 may not lead to significant passage effects in another [24]. Thus, the effects of prolonged
483 culture are complex and depend on the individual cell culture, tissue, and species.

484 The first criterion for identifying healthy and stable cells is observing cell morphology.
485 Chromosome content serves as another critical benchmark, as normal cells maintain a stable
486 chromosome number. Some studies using non-model species, such as felines [52] and fishes
487 [53], showed no heteroploidy on karyotypes obtained by cell cultures. However, to the best of
488 our knowledge, this is the first study that addresses genomic and chromosome changes in
489 wild birds and compares the effect of different cell passages on genome integrity.

490 Cryopreservation of cells has increasingly been considered a strategy for conservation as new
491 technologies using genetic material from somatic cells (e.g., somatic cell nuclear transfer or
492 induced pluripotent stem cells) are evolving [21,54]. One of the prerequisites for nuclear donor
493 cells and *ex situ* conservation is the stability of chromosomes [55]. Studies that investigate cell

494 line passage and age effects are still scarce in non-model organisms and are crucial since
495 altered metabolism and genomic instability no longer represent reliable models of their original
496 source of material.

497 Herein, comparison between karyotypes of passage 5 and passage 10 showed no differences,
498 suggesting that no large structural rearrangement occurred during the progressive number of
499 passages and that it is safe to establish the diploid number of (this) bird species until at least
500 the 10th passage. Genetic instability is well-documented in cells that have undergone more
501 than 20 passages, particularly in transformed continuous cell lines (e.g., [56]) and tumour cell
502 lines [57,58]. However, for primary cell cultures, a straightforward method to determine the
503 safest passage number before cells develop mutations or genetic instability is lacking. We
504 opted to cultivate cells up to passage 10 based on two factors: first, the uncertainty
505 surrounding the exact passage limit at which primary cells may enter senescence (as non-
506 continuous cell line has a limited *in vitro* life time); and second, technical challenges observed
507 during later passages as cells began to exhibit signs of morphological decline, including the
508 presence of granules and debris, difficulty detaching, and a reduced growth rate, all of which
509 would complicate further subculturing beyond passage 10. This seems to suggest rather safe
510 cell culturing for this species until passage 10. To some extent, this is supported by our SNP
511 analysis of several passage replicates which indicated no general pattern for increased
512 genomic changes between passages 5 and 10. However, we detected outlier samples with
513 respect to SNP numbers among replicates of both passage numbers. At this point, we lack
514 any point of reference expectation as to how many (potential) mutations are to be expected in
515 a cell culture system as the one we applied. Compared to overall levels of variant sites, the
516 number of SNPs in the individual samples which could be mutations is lower and represented
517 between 0.0039-0.0075 % of the genome assembly length. The effects of these variants
518 remain to be determined as well as the reason for between replicate differences. We further
519 suspect that several mutations are variant-calling artefacts, supported by lower SNP calling
520 quality, which asks for an exploration of mutation identification and more importantly validation

for the type of cell culture we have set up here.

Potential implications

We were able to assemble a reference genome for the Ural Owl of gold standard quality which is open to the community to be used for broader comparative genomic studies and phylogenomic analysis but also serves immediately to researchers interested in the Ural Owl for taxonomic and conservation aspects. With the data generated, we contribute to the endeavour of sequencing all life on Earth https://www.earthbiogenome.org/. Our analysis of genomic data derived from cell passages opens space for discussion of cell cultures as material for genomics especially for species with limited biological material available. The workflows applied by us could be used on similar data from other species.

Methods

Species origin and sampling strategy

Skin and muscle tissue samples from a ten-year-old male individual of *S. uralensis* (ring ID ZG-14.0-10-0234) were obtained from the Raptor Center & Wildlife Park Hellenthal (Wildfreigehege und Greifvogelstation Hellenthal, Hellenthal, Germany) during necropsy in 2020. The procedure was performed by Dominik Fischer, who is a veterinarian and approved to handle animals. No further approval was needed for this study. DNA barcoding was performed (collection ID ZFMK-TIS-50475) to ensure species identity using primers for COI from Astrin and Stüben [59] and sequences matched against BOLD (Barcode of Life Data System) [60]. The barcode sequence has been uploaded to BOLD as FOGS049-22.

Reference genome

Sequencing

DNA was extracted from the skin biopsy (collection ID ZFMK-TIS-50482, stored at LIB Biobank in liquid nitrogen vapor phase) using the Monarch HMW DNA Extraction Kit (NEB, Ipswich, USA). High-molecular weight status was validated by quality control with capillary electrophoresis (Agilent Femto Pulse) and a SPK 3.0 PacBio HiFi library was prepared according to the recommendations by the vendor. Next, HiFi SMRT sequencing was performed on two SMRT cells on a PacBio Sequel IIe (Pacific Biosciences, Menlo Park, USA) at the Max-Planck Genome-centre Cologne (MP-GC; Cologne, Germany). Also, a chromatin-capture library was prepared from cryopreserved cells generated for the analysis over progressive cell passages as described below with an Arima-Hi-C Kit according to the protocol for Mammalian Cell Lines followed by sequencing on an Illumina NextSeq 2000 in paired-end read mode.

Read processing

HiFi data

Contaminant sequences were filtered from the HiFi reads using Kraken2 v2.1.3 [61,62] with the Kraken database kraken2 PlusPFP downloaded in March 2023 and parameters "--confidence 0.51 --use-names". HiFi read quality was assessed using seqkit v2.8.2 [63,64] and a k-mer-based approach. K-mers were calculated with Meryl v1.4.1 [65] using the parameters "count k=21", and the counts were converted into a histogram with the *meryl histogram* command.

To verify the ploidy of the individual, Smudgeplot v0.2.5 [66] was used. First, k-mers within a specific range (lower-upper), determined with the *smudgeplot.py* cutoff function, were extracted using the meryl *print less-than* command. These filtered k-mers were then processed with *smudgeplot.py hetkmers* to calculate the coverage of unique heterozygous k-mer pairs. The resulting coverage was plotted using smudgeplot_plot.R.

GenomeScope2 v2.0.1 [66] was used to estimate genome size, heterozygosity, and the homozygous and heterozygous coverage peaks.

ROHan v1.0.1 [67] was used to identify large (>1 Mb) runs of homozygosity.

Hi-C data

Adapter removal and quality filtering of the raw Hi-C reads were performed using Fastp v0.23 [68] with parameters "--length_required 95, --qualified_quality_phred 20 --adapter_fasta", with a curated adapter list of the most common adapters used as input.

Error correction was done using *Tadpole* from BBMap v39.01 (https://sourceforge.net/projects/bbmap/), with parameters "k=50, reassemble=t, mode=correct, minprob=0.6, prefilter=1, prehashes=2, and prealloc=t". To remove contamination from the short, Hi-C reads, Kraken2 v2.1.3 was used similarly to the HiFi reads but in paired-read mode, with parameter "--paired".

Initial Genome Assembly

The HiFi reads were used with Hifiasm v0.19.5 [69] to generate a phased genome assembly. In order to obtain an optimal, phased genome we tested several Hifiasm parameters before choosing the ones that provided us with the assembly of the highest contiguity and completeness with both phased haplotypes having a similar length. We tested all possible combination of different purging level (0, 2, 3), increasing run-time, and number of iterations ("--n-weight 5 --n-perturb 50000 --f-perturb 0.5 -D 10 -N 150 -s 0.2") and explicitly providing the homozygous peak to Hifiasm which was estimated by GenomeScope ("--hom-cov 40") (for more details see Supplementary Table S1).

Genome Scaffolding

The selected haplomes from Hifiasm were split at positions containing Ns using *split_fa* from the Purge_Dups package v1.2.6 [70]. The resulting sequences were mapped to themselves using Minimap2 v2.26 [71] with parameters "-x asm5 -DP" and to the HiFi reads using Minimap2 with parameters "-x map-hifi". These mappings were used to remove assembly duplicates with Purge_Dups.

Mitochondrial Genome Detection

To identify and extract the mitochondrial genome, we utilized MitoHiFi v3.2.1 [72,73] referencing the sequence NC_038218.1 from *S. uralensis* (isolate C5 mitochondrial genome, complete, https://www.ncbi.nlm.nih.gov/nuccore/NC_038218.1). The most likely scaffold was kept and identified as the mitochondrial chromosome (MT) and all other candidate scaffolds were removed from the assembly.

Assembly Manual Curation

Hi-C reads were aligned to the final assemblies and a Hi-C contact map was created using PretextMap v0.0.2 (https://github.com/sanger-tol/PretextMap). A HiFi coverage track was generated from the aligned HiFi reads using bedtools *genomecov* and integrated into the Pretext map with *PretextGraph.*

Manual curation was performed within PretextView v0.0.2 (https://github.com/sanger-tol/PretextView), where scaffolds were reordered and oriented based on Hi-C interaction frequencies. Following curation, the final assembly scaffolds were processed with AGP tools from the Vertebrate Genomes Project (VGP) using the rapid manual curation protocol (https://gitlab.com/wtsi-grit/rapid-curation/-/tree/main) established by the Darwin Tree of Life consortium (https://www.darwintreeoflife.org/) to create the curated assembly. Scaffold names were further sorted and renamed by size using a combination of seqkit v2.8.2 and SAMtools v1.19.2 [74]. The final Hi-C contact map was visualized with HiCExplorer [75].

Genome Quality Control

The completeness of the final curated assembly was assessed using BUSCO v5.8 [76] and compleasm v0.2.6 [77] with the aves_odb10 lineage. Assembly contiguity and general assembly metrics were calculated using Quast v5.2.0 [78].

For k-mer-based analysis, k-mer counts were generated for each assembly using Meryl. These counts were analysed with Merqury v1.3 [79] to estimate assembly completeness and accuracy. The analysis yields Merqury's consensus QV, which is estimated by comparing the read and assembly k-mer counts and then transformed to a log-scaled probability of base-call errors. A higher QV indicates a more accurate assembly. We also obtained a Merqury completeness percent, which reflects the proportions of high-quality HiFi read k-mers present in the assembly.

HiFi reads were mapped to each assembly using Minimap2 with parameters “-ax map-hifi”. Alignment quality and coverage distribution were assessed using Qualimap v2.3 [80].

627 Potential contamination and quality was also assessed using the blobtoolkit pipeline v3.5.4
628 [81] and visualized using the interactive Blobtoolkit viewer in the Galaxy EU server [82] .

629 Genome Annotation

630 Repeat annotation

631 Repetitive elements in the primary assembly were identified and annotated using EarlGrey
632 v5.1.1 [83], which was run with RepeatMasker v4.1.5 [84] and RepeatModeler v2.0.6 [85]. In
633 addition to the RepeatModeler library, we used a previously-created, custom avian TE library
634 to mask repetitive elements [86]. The softmasked genome was used for protein-coding gene
635 prediction.

636 Protein-Coding Gene Annotation

637 To perform protein annotation, we created two reference protein sets. Set one contained only
638 the merged proteomes of the following publicly available genomes, downloaded using the
639 NCBI dataset cli v16.3.0 [87]*: S. nigrolineata* (GCA_013396715.1), *Gallus gallus*
640 (GCF_016699485.2), *Glaucidium brasilianum* (GCA_013399595.1), *Falco peregrinus*
641 (GCF_023634155.1), *Athene cunicularia* (GCF_003259725.1), *Aquila chrysaetos*
642 (GCF_900496995.4) [88], *Taeniopygia guttata* (GCF_003957565.2), and *Anas platyrhynchos*
643 (GCF_015476345.1).

644 Protein set two was created by merging all proteomes in set one with proteins from the
645 following public and curated databases: i) proteins from the BUSCO v5.4 aves_odb10 dataset,
646 ii) aves proteins from OrthoDB v11 [89] were obtained using Tomas Bruna's orthodb-clades
647 pipeline (https://github.com/tomasbruna/orthodb-clades) and iii) proteomes were also
648 extracted from the UniProt database for the following species: *Calypte anna* (UP000054308),
649 *Steatornis caripensis* (UP000516988), *Cnemophilus loriae* (UP000517678), *Dasyornis*
650 *broadbenti* (UP000521322), *Corythaixoides concolor* (UP000526942), *Irena cyanogastra*
651 (UP000530962), *Bucco capensis* (UP000534107), *Cephalopterus ornatus* (UP000543364),

652 *Molothrus ater* (UP000553862), *Ptilonorhynchus violaceus* (UP000584880), *Promerops cafer*
653 (UP000587587), *Vidua chalybeata* (UP000634236), and *Urocolius indicus* (UP000654395).

654 Protein-coding genes in the *S. uralensis* genome were annotated using a combination of *ab*
655 *initio*, protein similarity, and transcriptome-based protein prediction models. BRAKER3 v3.0.3
656 [90,91] was run in EP mode using the protein set two described above. GALBA v1.0.11.2 [92]
657 was run using protein set one to annotate genes. The outputs from GALBA and BRAKER3
658 v3.0.2 were combined using *TSEBRA* from the BRAKER3 package. To ensure high-quality
659 annotations, only the longest gene orthologs for each locus were retained using the
660 *agat_sp_keep_longest_isoform.pl* script from the AGAT package v1.4.1 [93].

661 Demographic History of *S. uralensis*

662 The demographic history of the Ural Owl was reconstructed using PSMC v0.6.5 as
663 implemented by [94]. Variants were called per chromosome using a combination of BCFtools
664 v1.21 [95] *mpileup* with parameters "-Q 30 -q 30" and bcftools call using the "-c" option. The
665 resulting VCF file was converted to a consensus fastq format using the *vcfutils.pl* vcf2fq script
666 with parameters "-d 10, -D 60, and -Q 30". The PSMC model was run with the following
667 parameters: -N25 -t15 -r5 -p "2+2+25*2+4+6" and 100 bootstraps, a generation time of 3 years
668 [96,97] and an assumed mutation rate of 4.6x10-9 [98,99].

669 Owl Genome Synteny

670 In order to identify the Z sex chromosome within our genome assembly and to assess the
671 synteny of different owl genomes we used the *GetTwoGenomeSyn.pl* built-in script of
672 NGenomeSyn [100] with options: "-MappingBin minimap2 -MinLenA 100000 -MinLenB
673 100000 -NumThreads 5 -MappingPara '-Lx asm5 --eqx -I 200G --MD -N 1'" to estimate
674 chromosome-scale alignments between *S. aluco*, *S. uralensis,* and *B. scandiacus.* We
675 visualized only contigs that mapped to the curated chromosomes of our genome with an
676 alignment length larger than 1,000 bp.

677 # Functional Gene Annotation

678 Predicted genes were functionally annotated by performing sequence similarity searches
679 against the Swiss-Prot database using *BLASTP* from BLAST v2.13.0+ with default
680 parameters. As with our own genome's annotation, we used
681 *agat_sp_keep_longest_isoform.pl* to only keep the longest isoform of each gene locus from
682 the *Aquila chrysaetos, Gallus gallus, S. nigrolineata*, *Athene cunicularia, Glaucidium*
683 *brasilianum, Falco peregrinus,* proteomes of protein set one together with *Tyto alba*
684 (GCA_018691265.1) and *Haliaeetus leucocephalus* (GCA_000737465.1) and used
685 OrthoFinder v2.5.5 [101] to estimate orthologous gene families among those species. This
686 analysis identified orthogroups and genes that have undergone expansion or contraction in
687 the Ural Owl, as well as orthogroups unique to this species.

688 # Gene Ontology Term Analysis

689 Gene Ontology Term analysis was performed by mapping all Ural Owl genes to the Vertebrate
690 Eggnog database using eggnog mapper v2.1.12 [102,103]. Missing GO Terms were filled in
691 with the GO Terms of the previously found Swiss-Prot gene symbols associated with each
692 gene. Next, the genes belonging to gene families unique to the Ural Owl (found with
693 Orthofinder) were analysed by Revigo v1.8.1 [104] with default settings and choosing the
694 *Large* subset option. The resulting GO Terms were analysed with Revigo again with default
695 settings and this time with the *Small* subset option. The full *Biological Process* Revigo table
696 was plotted in R v4.4.2 using an edited version of the Revigo treemap plotting script.

697 # Variation analysis over progressive cell passages

698 ## Cell Culture

699 Primary cells were grown from a skin biopsy of the same individual as used for genome
700 sequencing (collection ID ZFMK-TIS-51054) previously stored at LIB Biobank in liquid

701 nitrogen, following standard protocols. Skin tissues were rapidly thawed, minced into small
702 fragments, and transferred to cell culture flasks. Flasks were incubated at 37°C with 5 % CO_2
703 in Fibroblast Growth Basal Medium (FBM; Lonza, Cologne, Germany) supplemented with 20%
704 Fetal Bovine Serum (FBS; Biowest, Nuaillé, France) including antibiotics (100 U/mL penicillin
705 and 100 g/mL streptomycin; Sigma-Aldrich, St. Louis, United States). Cells were visually
706 inspected in inverted microscope Nikon Eclipse TS2 for contamination and cell media was
707 changed every 2-3 days. After reaching ~80 % confluence (determined visually), cells were
708 propagated using 0.125 % trypsin solution (Biowest), at subculture ratio 50:50. Cells were
709 harvested for DNA extraction and chromosome analysis at passages 5 (three different
710 replicates) and passage 10 (four different replicates).

711 Chromosome sampling for large variant analysis

712 In order to investigate the stability of the karyotype composition through different passages,
713 chromosome preparations were obtained from cells for passages 5 and 10, according to [105],
714 with modifications. Chromosomes were harvested after treatment with colchicine 0.01% for
715 one hour, followed by hypotonic treatment with 0.075 M KCl, and cell fixation in methanol /
716 acetic acid (3:1). Slides were stained with Giemsa 5 %. At least 20 metaphases for each
717 passage were analysed to define the diploid number (2n) in a Zeiss microscope Axio Imager
718 Z2m.

719 DNA extraction of primary tissue and cell culture passages

720 Passage samples were extracted using the DNeasy Blood & Tissue Kit (Qiagen, Hilden,
721 Germany) following the manufacturer's protocol for cultured cells, while muscle tissue of the
722 same individual (collection ID ZFMK-TIS-50476) previously stored at LIB Biobank in 96 %
723 ethanol (passage 0) was extracted using the standard protocol of the same kit.

724 ## Sequencing of primary tissue and passages

725 After DNA extraction, samples were sent for purification (Vahtstm DNA Clean Beads; Vazyme
726 Biotech, Nanjing, China), PCR-free library preparation (NEBNext Ultra II FS DNA PCR-free
727 Library Prep Kit for Illumina; NEB) and subsequent paired-end sequencing on a NovaSeq
728 6000 (Illumina, San Diego, USA) using the NovaSeq 6000 S4 Reagent Kit (Illumina) to
729 Biomarker Technologies (bmkgene; Beijing, China).

730 ## Read Mapping

731 The Illumina reads of all passages (passage 0, i.e. the primary tissue, three passage 5
732 replicate samples and four passage 10 replicate samples) were processed with fastp v0.20.0
733 [68] with parameters "--length_required 95, --qualified_quality_phred 20 --adapter_fasta", with
734 a curated adapter list of the most common adapters used as input and decontaminated with
735 Kraken2 v2.1.3 with the Kraken database kraken2 PlusPFP database downloaded in March
736 2023 in paired-read mode, with parameter "--paired --confidence 0.51 --use-names". These
737 reads were then mapped to the reference genome using BWA-MEM2 v2.2.1 [106,107] with
738 the *mem* command and options "-M -R", where a read group (RG) specific to each sample
739 was used for "-R". The resulting output was sorted using SAMtools v1.19.2, and additional
740 processing steps (SAMtools' *fixmate*, *sort*, and *markdup*) were performed to generate the final
741 mapping files for each sample.

742 ## SNP Calling

743 SNP calling for each cell passage sample and the HiFi reads ("reference") was performed
744 individually using GATK HaplotypeCaller v4.2.6.1 [108,109] with the options "-ERC GVCF --
745 min-base-quality-score 30 --pcr-indel-model NONE". Joint SNP calling was performed by first
746 combining samples using GATK *GenomicsDBImport* with the option "--batch-size 3". The
747 combined database was then used for joint SNP calling with GATK's *GenotypeGVCFs*.

748 Variant quality recalibration was conducted in three rounds. GATK's *BaseRecalibrator* was

run with the option “--maximum-cycle-value 50000”, followed by GATK’s *ApplyBQSR* for each sample before re-calling variants individually and collectively. From the final set of called genotypes, SNPs were extracted using GATK’s *SelectVariants* with the option “-select-type SNP” and filtered with GATK VariantFiltration using the filters: “QD < 2.0, FS > 60.0, MQ < 40.0, SOR > 3.0, MQRankSum < -12.5, ReadPosRankSum < -8.0, QUAL < 30.0”.

Variants were filtered for depth, minor allele frequency (MAF) and the fraction of missing genotypes using BCFtools filter v1.21 (https://github.com/samtools/bcftools) with the options “-e "INFO/DP<$MIN_DEPTH || INFO/DP>$MAX_DEPTH" ” and “-i "MAF>$MAF && F_MISSING<=$MISS".

Short-read variant analysis in passages

To assess the quality of the DNA contained in cell cultures and to understand its potential for being used as an amplified genomic resource, these filtered SNPs were then analysed in R v4.4.2. Passages 5 and 10 were compared to passage 0 and the HiFi reads at sites where passages 5 and 10 differ from either of the reference passages. A Wilcoxon test from rstatix v0.7.2 was performed to test whether the depth and GQ of these SNPs of each sample were significantly different from the average DP or GQ. The variant calls were re-coded so that: "0|0" = 0, "0|1" = 1, "1|0" = 1, "1|1" = 2, "0|2" = 3, "2|0" = 3, "1|2" = 4, "2|1" = 4, "2|2" = 5, "0|3" = 6, "3|0" = 6 and plotted with ggplot2.

Availability of source code and requirements

Project: Strix uralensis assembly, annotation and comparative analysis

Location: Zenodo DOI: 10.5281/zenodo.15100180

Operating system(s): e.g. Platform independent

Licence: CC0

Data Availability

The sequencing reads, assembly and BioSample data supporting the results of this article are available in the INSDC under the BioProject number PRJNA1212906. Further datasets and code supporting the results of this article are available from Zenodo under DOI: 10.5281/zenodo.14676512. Code is available from Zenodo under DOI: 10.5281/zenodo.15100180.

List of abbreviations

2n: diploid chromosome number; b: bases; bp: base pair; BLAST: basic local alignment search tool; BOLD: Barcode of Life Data System; BUSCO: Benchmarking Universal Single-Copy Orthologs; C: Celsius; CBD: convention on biological diversity; CITES: convention on international trade in endangered species of wild fauna and flora; DP: depth; EU: European Union; FBS: Fetal Bovine Serum; GATK: Genome Analysis Toolkit; Gb: gigabases; GO: gene ontology; GQ: genotype quality; Hi-C: high-throughput chromosome conformation capture; HiFi: high-fidelity; HMW: high molecular weight; INSDC: International Nucleotide Sequence Database Collaboration; kb: kilobases; LINE: long interspersed nuclear element; LTR: long terminal repeat transposable element; M: molar; MAF: major allele frequency; Mb: megabases; MT: mitochondrial chromosome; PSMC: Pairwise Sequentially Markovian Coalescent; QV: quality value; RG: read group; ROH: runs of homozygosity; SNP: single nucleotide polymorphism; TE; transposable element; VCF: variant call format; VGP: Vertebrate Genomes Project; ya: years ago.

Declarations

The primary tissue used for this work was derived from a naturally deceased bird and provided by a veterinarian. We did not perform animal experimentation.

Competing Interests

The authors declare that they have no competing interests.

Funding

This work was supported by the Leibniz Gemeinschaft Leibniz Association Network grant CollOmic K419/2021 to AB and LIB innovation fund to AB and JJA.

Authors' contributions

IC: conceptualization, data curation, formal analysis, investigation, methodology, software, validation, visualization, writing (original draft; review & editing); AM: conceptualization, data curation, formal analysis, investigation, methodology, validation, visualization, writing (original draft; review & editing); CBDN: conceptualization, formal analysis, investigation, methodology, writing (original draft; review & editing); DF: resources, writing (review & editing); NS: investigation, writing (review & editing); LvdM: investigation, writing (review & editing); BH: investigation, writing (review & editing); JJA: conceptualization, funding acquisition, supervision, writing (original draft; review & editing); TT: validation, supervision, writing (original draft; review & editing); AB: conceptualization, data curation, validation, visualization, funding acquisition, supervision, writing (original draft; review & editing).

Acknowledgements

We thank Juliane Vehof and Benjamin Wipfler for enabling us to use their microscope.

References

1. Ellegren H. Evolutionary stasis: the stable chromosomes of birds. *Trends Ecol Evol*. 2010; doi: 10.1016/j.tree.2009.12.004.

2. Rebholz WER, Boer LEMD, Sasaki M, Belterman RHR, Nishida-Umehara C. The chromosomal phylogeny of owls (Strigiformes) and new karyotypes of seven species. *Cytologia (Tokyo)*. 1993; doi: 10.1508/cytologia.58.403.

3. Burt DW. Origin and evolution of avian microchromosomes. *Cytogenet Genome Res*. 2002; doi: 10.1159/000063018.

4. Pichugin AM, Galkina SA, Potekhin AA, Punina EO, Rautian MS, Rodionov AV. Estimation of the minimal size of chicken *Gallus gallus domesticus* microchromosomes via pulsed-field electrophoresis. *Russ J Genet*. 2001; doi: 10.1023/A:1016622816552.

5. Degrandi TM, Barcellos SA, Costa AL, Garnero ADV, Hass I, Gunski RJ. Introducing the bird chromosome database: An overview of cytogenetic studies in birds. *Cytogenet Genome Res*. 2020; doi: 10.1159/000507768.

6. Smith J, Bruley CK, Paton IR, Dunn I, Jones CT, Windsor D, et al.. Differences in gene density on chicken macrochromosomes and microchromosomes. *Anim Genet*. 2000; doi: 10.1046/j.1365-2052.2000.00565.x.

7. Axelsson E, Webster MT, Smith NGC, Burt DW, Ellegren H. Comparison of the chicken and turkey genomes reveals a higher rate of nucleotide divergence on microchromosomes than macrochromosomes. *Genome Res*. 2005; doi: 10.1101/gr.3021305.

8. Roselaar C. Strix uralensis Ural Owl. In: Cramp S, editor. *Handb Birds Eur Middle East North Afr Birds West Paleartic*. Oxford University Press; p. 550–60.

9. Able KP. Handbook of the Birds of the World, Volume 5, Barn-owls to Hummingbirds. *The Auk*. 2000; doi: 10.1093/auk/117.2.532.

10. Hausknecht R, Jacobs S, Müller J, Zink R, Frey H, Solheim R, et al.. Phylogeographic analysis and genetic cluster recognition for the conservation of Ural Owls (*Strix uralensis*) in Europe. *J Ornithol*. 2014; doi: 10.1007/s10336-013-0994-8.

11. Cramp S. Handbook of the birds of Europe, the Middle East, and north Africa: the birds of the western Paleartic. Oxford London New York: Oxford university press;

12. König C, Weick F. Owls of the World (2nd ed.). Helm identification Guides. A & C Black Publishers Ltd.;

13. Mikkola H, Willis I. Owls of Europe. Calton, Waterhouses, Staffordshire, England: T & A D Poyser;

14. IUCN. Strix uralensis: Westrip, J.R.S. & BirdLife International: The IUCN Red List of Threatened Species 2022: e.T22689108A209840432.

15. Kopij G. Population and range expansion of forest boreal owls (*Glaucidium passerinum, Aegolius funereus, Strix uralensis, Strix nebulosa*) in East-Central Europe. *Vogelwelt*. 132:207–142011;

16. Scherzinger W. Die Wiederbegründung des Habichtskauz-Vorkommens *Strix uralensis* im Böhmerwald. *Ornithol Anz*. 45:97–1562006;

17. Soorae PS. Global re-introduction perspectives, 2011: more case studies from around the globe. Abu Dhabi, UAE: IUCN/SSC Re-introduction Specialist Group & Environment Agency - Abu Dhabi;

18. Scope A, Schwendenwein I, Stanclova G, Vobornik A, Zink R. Exploratory plasma biochemistry reference intervals for Ural Owls (*Strix uralensis*, Pallas 1771) from the Austrian reintroduction project. *J Zoo Wildl Med*. 2016; doi: 10.1638/2015-0200.1.

19. Huntley B, Green R, Collingham YC, Willis SG. A climatic atlas of european breeding birds. Barcelona: Lynx ed;

20. Lehikoinen A, Ranta E, Pietiäinen H, Byholm P, Saurola P, Valkama J, et al.. The impact of climate and cyclic food abundance on the timing of breeding and brood size in four boreal owl species. *Oecologia*. 2011; doi: 10.1007/s00442-010-1730-1.

21. Mooney A, Ryder OA, Houck ML, Staerk J, Conde DA, Buckley YM. Maximizing the potential for living cell banks to contribute to global conservation priorities. *Zoo Biol*. 2023; doi: 10.1002/zoo.21787.

22. Ryder OA, Onuma M. Viable cell culture banking for biodiversity characterization and

874 conservation. *Annu Rev Anim Biosci*. 2018; doi: 10.1146/annurev-animal-030117-014556.
875 23. Freshney RI. Culture of animal cells: a manual of basic technique and specialized
876 applications. 6th edition. John Wiley & Sons;
877 24. Hughes P, Marshall D, Reid Y, Parkes H, Gelber C. The costs of using unauthenticated,
878 over-passaged cell lines: How much more data do we need? *BioTechniques*. Taylor &
879 Francis; 2007; doi: 10.2144/000112598.
880 25. Yamada K, Nishida-Umehara C, Matsuda Y. A new family of satellite DNA sequences as
881 a major component of centromeric heterochromatin in owls (Strigiformes). *Chromosoma*.
882 2004; doi: 10.1007/s00412-003-0267-z.
883 26. Takagi N, Sasaki M. A phylogenetic study of bird karyotypes. *Chromosoma*. 1974; doi:
884 10.1007/BF00332341.
885 27. Feng S, Stiller J, Deng Y, Armstrong J, Fang Q, Reeve AH, et al.. Dense sampling of
886 bird diversity increases power of comparative genomics. *Nature*. 2020; doi: 10.1038/s41586-
887 020-2873-9.
888 28. Baalsrud HT, Garmann-Aarhus B, Enevoldsen ELG, Krabberød AK, Fischer D, Tooming-
889 Klunderud A, et al.. Evolutionary new centromeres in the snowy owl genome putatively
890 seeded from a transposable element.
891 29. Forest T, Achaz G, Marbouty M, Bignaud A, Thierry A, Koszul R, et al.. Chromosome-
892 level genome assembly of the European green woodpecker *Picus viridis*. Campbell P, editor.
893 *G3 Genes Genomes Genet*. 2024; doi: 10.1093/g3journal/jkae042.
894 30. Kapusta A, Suh A, Feschotte C. Dynamics of genome size evolution in birds and
895 mammals. *Proc Natl Acad Sci*. Proceedings of the National Academy of Sciences; 2017; doi:
896 10.1073/pnas.1616702114.
897 31. Tegelström H, Ryttman H. Chromosomes in birds (Aves): evolutionary implications of
898 macro-and microchromosome numbers and lengths. *Hereditas*. 1981; doi: 10.1111/j.1601-
899 5223.1981.tb01757.x.
900 32. Fillon V. The chicken as a model to study microchromosomes in birds: a review. *Genet*
901 *Sel Evol*. 1998; doi: 10.1186/1297-9686-30-3-209.

902 33. McQueen HA, Fantes J, Cross SH, Clark VH, Archibald AL, Bird AP. CpG islands of
903 chicken are concentrated on microchromosomes. *Nat Genet*. 1996; doi: 10.1038/ng0396-
904 321.
905 34. Schmid M, Nanda I, Guttenbach M, Steinlein C, Hoehn M, Schartl M, et al.. First report
906 on chicken genes and chromosomes 2000. *Cytogenet Genome Res*. 2000; doi:
907 10.1159/000056772.
908 35. International Chicken Genome Sequencing Consortium. Sequence and comparative
909 analysis of the chicken genome provide unique perspectives on vertebrate evolution. *Nature*.
910 2004; doi: 10.1038/nature03154.
911 36. Waters PD, Patel HR, Ruiz-Herrera A, Álvarez-González L, Lister NC, Simakov O, et al..
912 Microchromosomes are building blocks of bird, reptile, and mammal chromosomes. *Proc*
913 *Natl Acad Sci*. 2021; doi: 10.1073/pnas.2112494118.
914 37. Borges R, Khan I, Johnson WE, Gilbert MTP, Zhang G, Jarvis ED, et al.. Gene loss,
915 adaptive evolution and the co-evolution of plumage coloration genes with opsins in birds.
916 *BMC Genomics*. 2015; doi: 10.1186/s12864-015-1924-3.
917 38. Greenwold MJ, Bao W, Jarvis ED, Hu H, Li C, Gilbert MTP, et al.. Dynamic evolution of
918 the alpha (α) and beta (β) keratins has accompanied integument diversification and the
919 adaptation of birds into novel lifestyles. *BMC Evol Biol*. 2014; doi: 10.1186/s12862-014-
920 0249-1.
921 39. Wagner H, Weger M, Klaas M, Schröder W. Features of owl wings that promote silent
922 flight. *Interface Focus*. 2017; doi: 10.1098/rsfs.2016.0078.
923 40. Luo H, Lin Q, Fang W, Chen X, Zhou X. Genomic insights into the endangered white-
924 eared night heron (*Gorsachius magnificus*). *BMC Genomic Data*. 2024; doi:
925 10.1186/s12863-024-01194-1.
926 41. Robinson JA, Bowie RCK, Dudchenko O, Aiden EL, Hendrickson SL, Steiner CC, et al..
927 Genome-wide diversity in the California condor tracks its prehistoric abundance and decline.
928 *Curr Biol*. 2021; doi: 10.1016/j.cub.2021.04.035.
929 42. Li S, Li B, Cheng C, Xiong Z, Liu Q, Lai J, et al.. Genomic signatures of near-extinction

and rebirth of the crested ibis and other endangered bird species. *Genome Biol*. 2014; doi: 10.1186/s13059-014-0557-1.

43. Li B-P, Kang N, Xu Z-X, Luo H-R, Fan S-Y, Ao X-H, et al.. Transposable elements shape the landscape of heterozygous structural variation in a bird genome. *Zool Res*. 2025; doi: 10.24272/j.issn.2095-8137.2024.237.

44. Pellegrino I, Negri A, Boano G, Cucco M, Kristensen TN, Pertoldi C, et al.. Evidence for strong genetic structure in European populations of the little owl *Athene noctua*. *J Avian Biol*. 2015; doi: 10.1111/jav.00679.

45. Brito PH. Contrasting patterns of mitochondrial and microsatellite genetic structure among Western European populations of tawny owls (*Strix aluco*). *Mol Ecol*. 2007; doi: 10.1111/j.1365-294X.2007.03401.x.

46. Antoniazza S, Burri R, Fumagalli L, Goudet J, Roulin A. Local adaptation maintains clinal variation in melanin-based coloration of European barn owls (*Tyto alba*). *Evolution*. 2010; doi: 10.1111/j.1558-5646.2010.00969.x.

47. Mueller JC, Kuhl H, Boerno S, Tella JL, Carrete M, Kempenaers B. Evolution of genomic variation in the burrowing owl in response to recent colonization of urban areas. *Proc R Soc B Biol Sci*. 2018; doi: 10.1098/rspb.2018.0206.

48. Spielman D, Brook BW, Frankham R. Most species are not driven to extinction before genetic factors impact them. *Proc Natl Acad Sci*. 2004; doi: 10.1073/pnas.0403809101.

49. Novenko EYu, Seifert-Eulen M, Boettger T, Junge FW. Eemian and Early Weichselian vegetation and climate history in Central Europe: A case study from the Klinge section (Lusatia, eastern Germany). *Rev Palaeobot Palynol*. 2008; doi: 10.1016/j.revpalbo.2008.02.005.

50. Velichko AA, Novenko EY, Pisareva VV, Zelikson EM, Boettger T, Junge FW. Vegetation and climate changes during the Eemian interglacial in Central and Eastern Europe: comparative analysis of pollen data. *Boreas*. 2008; doi: 10.1111/j.1502-3885.2005.tb01016.x.

51. Malkiewicz M. A Late Saalian Glaciation, Eemian Interglacial and Early Weichselian

958 pollen sequence at Szklarka, SW Poland – Reconstruction of vegetation and climate. *Quat*
959 *Int*. 2018; doi: 10.1016/j.quaint.2016.09.026.
960 52. Song J, Hua S, Song K, Zhang Y. Culture, characteristics and chromosome complement
961 of Siberian tiger fibroblasts for nuclear transfer. *Vitro Cell Dev Biol - Anim*. 2007; doi:
962 10.1007/s11626-007-9043-3.
963 53. Alvarez MC, Otis J, Amores A, Guise K. Short-term cell culture technique for obtaining
964 chromosomes in marine and freshwater fish. *J Fish Biol*. John Wiley & Sons, Ltd; 1991; doi:
965 10.1111/j.1095-8649.1991.tb04411.x.
966 54. Bolton RL, Mooney A, Pettit MT, Bolton AE, Morgan L, Drake GJ, et al.. Resurrecting
967 biodiversity: advanced assisted reproductive technologies and biobanking. *Reprod Fertil*.
968 Bristol, UK: Bioscientifica Ltd; 2022; doi: 10.1530/RAF-22-0005.
969 55. Song J, Hua S, Song K, Zhang Y. Culture, characteristics and chromosome complement
970 of Siberian tiger fibroblasts for nuclear transfer. *Vitro Cell Dev Biol - Anim*. 2007; doi:
971 10.1007/s11626-007-9043-3.
972 56. Odoemelam E, Raghavan N, Miller A, Bridger JM, Knight M. Revised karyotyping and
973 gene mapping of the *Biomphalaria glabrata* embryonic (Bge) cell line. *Int J Parasitol*. 2009;
974 doi: 10.1016/j.ijpara.2008.11.011.
975 57. He Z, Wilson A, Rich F, Kenwright D, Stevens A, Low YS, et al.. Chromosomal instability
976 and its effect on cell lines. *Cancer Rep*. John Wiley & Sons, Ltd; 2023; doi:
977 10.1002/cnr2.1822.
978 58. Wenger SL, Senft JR, Sargent LM, Bamezai R, Bairwa N, Grant SG. Comparison of
979 established cell lines at different passages by karyotype and comparative genomic
980 hybridization. *Biosci Rep*. 2005; doi: 10.1007/s10540-005-2797-5.
981 59. Astrin JJ, Stüben PE. Phylogeny in cryptic weevils: molecules, morphology and new
982 genera of western Palaearctic Cryptorhynchinae (Coleoptera: Curculionidae). *Invertebr Syst*.
983 2008; doi: 10.1071/IS07057.
984 60. Ratnasingham S, Hebert PDN. BOLD : The Barcode of Life Data System
985 (http://www.barcodinglife.org). *Mol Ecol Notes*. 2007; doi: 10.1111/j.1471-

986 8286.2007.01678.x.
987 61. Wood DE, Salzberg SL. Kraken: ultrafast metagenomic sequence classification using
988 exact alignments. *Genome Biol*. 2014; doi: 10.1186/gb-2014-15-3-r46.
989 62. Wood DE, Lu J, Langmead B. Improved metagenomic analysis with Kraken 2. *Genome*
990 *Biol*. 2019; doi: 10.1186/s13059-019-1891-0.
991 63. Shen W, Le S, Li Y, Hu F. SeqKit: A Cross-Platform and Ultrafast Toolkit for FASTA/Q
992 File Manipulation. Zou Q, editor. *PLOS ONE*. 2016; doi: 10.1371/journal.pone.0163962.
993 64. Shen W, Sipos B, Zhao L. SeqKit2: A Swiss army knife for sequence and alignment
994 processing. *iMeta*. 2024; doi: 10.1002/imt2.191.
995 65. Miller JR, Delcher AL, Koren S, Venter E, Walenz BP, Brownley A, et al.. Aggressive
996 assembly of pyrosequencing reads with mates. *Bioinformatics*. 2008; doi:
997 10.1093/bioinformatics/btn548.
998 66. Ranallo-Benavidez TR, Jaron KS, Schatz MC. GenomeScope 2.0 and Smudgeplot for
999 reference-free profiling of polyploid genomes. *Nat Commun*. 2020; doi: 10.1038/s41467-020-
1000 14998-3.
1001 67. Renaud G, Hanghøj K, Korneliussen TS, Willerslev E, Orlando L. Joint estimates of
1002 heterozygosity and runs of homozygosity for modern and ancient samples. *Genetics*. 2019;
1003 doi: 10.1534/genetics.119.302057.
1004 68. Chen S, Zhou Y, Chen Y, Gu J. fastp : an ultra-fast all-in-one FASTQ preprocessor.
1005 *Bioinforma Oxf Engl*. 2018; doi: 10.1093/bioinformatics/bty560.
1006 69. Cheng H, Concepcion GT, Feng X, Zhang H, Li H. Haplotype-resolved de novo
1007 assembly using phased assembly graphs with hifiasm. *Nat Methods*. 2021; doi:
1008 10.1038/s41592-020-01056-5.
1009 70. Guan D, McCarthy SA, Wood J, Howe K, Wang Y, Durbin R. Identifying and removing
1010 haplotypic duplication in primary genome assemblies. Valencia A, editor. *Bioinformatics*.
1011 2020; doi: 10.1093/bioinformatics/btaa025.
1012 71. Li H. Minimap2: pairwise alignment for nucleotide sequences. *Bioinformatics*. 2018; doi:
1013 10.1093/bioinformatics/bty191.

1014 72. Uliano-Silva M, Ferreira JGRN, Krasheninnikova K, Darwin Tree of Life Consortium,
1015 Blaxter M, Mieszkowska N, et al.. MitoHiFi: a python pipeline for mitochondrial genome
1016 assembly from PacBio high fidelity reads. *BMC Bioinformatics*. 2023; doi: 10.1186/s12859-
1017 023-05385-y.
1018 73. Allio R, Schomaker-Bastos A, Romiguier J, Prosdocimi F, Nabholz B, Delsuc F.
1019 MitoFinder: Efficient automated large-scale extraction of mitogenomic data in target
1020 enrichment phylogenomics. *Mol Ecol Resour*. 2020; doi: 10.1111/1755-0998.13160.
1021 74. Li H, Handsaker B, Wysoker A, Fennell T, Ruan J, Homer N, et al.. The Sequence
1022 Alignment/Map format and SAMtools. *Bioinformatics*. 2009; doi:
1023 10.1093/bioinformatics/btp352.
1024 75. Wolff J, Rabbani L, Gilsbach R, Richard G, Manke T, Backofen R, et al.. Galaxy
1025 HiCExplorer 3: a web server for reproducible Hi-C, capture Hi-C and single-cell Hi-C data
1026 analysis, quality control and visualization. *Nucleic Acids Res*. 2020; doi:
1027 10.1093/nar/gkaa220.
1028 76. Manni M, Berkeley MR, Seppey M, Simão FA, Zdobnov EM. BUSCO update: Novel and
1029 streamlined workflows along with broader and deeper phylogenetic coverage for scoring of
1030 eukaryotic, prokaryotic, and viral genomes. Kelley J, editor. *Mol Biol Evol*. 2021; doi:
1031 10.1093/molbev/msab199.
1032 77. Huang N, Li H. compleasm: a faster and more accurate reimplementation of BUSCO.
1033 Marschall T, editor. *Bioinformatics*. 2023; doi: 10.1093/bioinformatics/btad595.
1034 78. Gurevich A, Saveliev V, Vyahhi N, Tesler G. QUAST: quality assessment tool for
1035 genome assemblies. *Bioinformatics*. 2013; doi: 10.1093/bioinformatics/btt086.
1036 79. Rhie A, Walenz BP, Koren S, Phillippy AM. Merqury: reference-free quality,
1037 completeness, and phasing assessment for genome assemblies. *Genome Biol*. 2020; doi:
1038 10.1186/s13059-020-02134-9.
1039 80. Okonechnikov K, Conesa A, García-Alcalde F. Qualimap 2: advanced multi-sample
1040 quality control for high-throughput sequencing data. *Bioinformatics*. 2016; doi:
1041 10.1093/bioinformatics/btv566.

1042 81. Challis R, Richards E, Rajan J, Cochrane G, Blaxter M. BlobToolKit – Interactive Quality
1043 Assessment of Genome Assemblies. *G3 GenesGenomesGenetics*. 2020; doi:
1044 10.1534/g3.119.400908.
1045 82. Afgan E, Baker D, Batut B, van den Beek M, Bouvier D, Čech M, et al.. The Galaxy
1046 platform for accessible, reproducible and collaborative biomedical analyses: 2018 update.
1047 *Nucleic Acids Res*. 2018; doi: 10.1093/nar/gky379.
1048 83. Baril T, Galbraith J, Hayward A. Earl Grey: A fully automated user-friendly transposable
1049 element annotation and analysis pipeline. *Mol Biol Evol*. 2024; doi:
1050 10.1093/molbev/msae068.
1051 84. Tarailo-Graovac M, Chen N. Using RepeatMasker to identify repetitive elements in
1052 genomic sequences. *Curr Protoc Bioinforma*. 2009; doi: 10.1002/0471250953.bi0410s25.
1053 85. Flynn JM, Hubley R, Goubert C, Rosen J, Clark AG, Feschotte C, et al.. RepeatModeler2
1054 for automated genomic discovery of transposable element families. *Proc Natl Acad Sci*.
1055 2020; doi: 10.1073/pnas.1921046117.
1056 86. Kapusta A, Suh A. Evolution of bird genomes—a transposon's-eye view. *Ann N Y Acad*
1057 *Sci*. 2017; doi: 10.1111/nyas.13295.
1058 87. O'Leary NA, Cox E, Holmes JB, Anderson WR, Falk R, Hem V, et al.. Exploring and
1059 retrieving sequence and metadata for species across the tree of life with NCBI Datasets. *Sci*
1060 *Data*. 2024; doi: 10.1038/s41597-024-03571-y.
1061 88. Mead D, Ogden R, Meredith A, Peniche G, Smith M, Corton C, et al.. The genome
1062 sequence of the European golden eagle, *Aquila chrysaetos chrysaetos* Linnaeus 1758.
1063 *Wellcome Open Res*. 2021; doi: 10.12688/wellcomeopenres.16631.1.
1064 89. Kriventseva EV, Tegenfeldt F, Petty TJ, Waterhouse RM, Simão FA, Pozdnyakov IA, et
1065 al.. OrthoDB v8: update of the hierarchical catalog of orthologs and the underlying free
1066 software. *Nucleic Acids Res*. 2015; doi: 10.1093/nar/gku1220.
1067 90. Gabriel L, Brůna T, Hoff KJ, Ebel M, Lomsadze A, Borodovsky M, et al.. BRAKER3: Fully
1068 automated genome annotation using RNA-seq and protein evidence with GeneMark-ETP,
1069 AUGUSTUS and TSEBRA.

1070 91. Hoff KJ, Lange S, Lomsadze A, Borodovsky M, Stanke M. BRAKER1: Unsupervised
1071 RNA-seq-based genome annotation with GeneMark-ET and AUGUSTUS. *Bioinformatics*.
1072 2016; doi: 10.1093/bioinformatics/btv661.
1073 92. Brůna T, Li H, Guhlin J, Honsel D, Herbold S, Stanke M, et al.. Galba: genome
1074 annotation with miniprot and AUGUSTUS. *BMC Bioinformatics*. 2023; doi: 10.1186/s12859-
1075 023-05449-z.
1076 93. Jacques Dainat, Darío Hereñú, Dr. K. D. Murray, Ed Davis, Ivan Ugrin, Kathryn Crouch,
1077 et al.. NBISweden/AGAT: AGAT-v1.4.1. Zenodo;
1078 94. Li H, Durbin R. Inference of human population history from individual whole-genome
1079 sequences. *Nature*. 2011; doi: 10.1038/nature10231.
1080 95. Danecek P, Auton A, Abecasis G, Albers CA, Banks E, DePristo MA, et al.. The variant
1081 call format and VCFtools. *Bioinformatics*. 2011; doi: 10.1093/bioinformatics/btr330.
1082 96. Béziers P, Roulin A. Sexual maturity varies with melanic plumage traits in the barn owl. *J*
1083 *Avian Biol*. 2021; doi: 10.1111/jav.02715.
1084 97. Brommer JE, Pietiäinen H, Kolunen H. Reproduction and survival in a variable
1085 environment: Ural owls (*Strix uralensis*) and the three-year vole cycle. Marti C, editor. *The*
1086 *Auk*. 2002; doi: 10.1093/auk/119.2.544.
1087 98. Fujito NT, Hanna ZR, Levy-Sakin M, Bowie RCK, Kwok P-Y, Dumbacher JP, et al..
1088 Genomic variation and recent population histories of Spotted (*Strix occidentalis*) and Barred
1089 (*Strix varia*) Owls. Lohmueller K, editor. *Genome Biol Evol*. 2021; doi: 10.1093/gbe/evab066.
1090 99. Terhorst J, Kamm JA, Song YS. Robust and scalable inference of population history
1091 from hundreds of unphased whole genomes. *Nat Genet*. 2017; doi: 10.1038/ng.3748.
1092 100. He W, Yang J, Jing Y, Xu L, Yu K, Fang X. NGenomeSyn: an easy-to-use and flexible
1093 tool for publication-ready visualization of syntenic relationships across multiple genomes.
1094 Marschall T, editor. *Bioinformatics*. 2023; doi: 10.1093/bioinformatics/btad121.
1095 101. Emms DM, Kelly S. OrthoFinder: phylogenetic orthology inference for comparative
1096 genomics. *Genome Biol*. 2019; doi: 10.1186/s13059-019-1832-y.
1097 102. Cantalapiedra CP, Hernández-Plaza A, Letunic I, Bork P, Huerta-Cepas J. eggNOG-

1098 mapper v2: Functional annotation, orthology assignments, and domain prediction at the
1099 metagenomic scale. Tamura K, editor. *Mol Biol Evol*. 2021; doi: 10.1093/molbev/msab293.
1100 103. Huerta-Cepas J, Szklarczyk D, Heller D, Hernández-Plaza A, Forslund SK, Cook H, et
1101 al.. eggNOG 5.0: a hierarchical, functionally and phylogenetically annotated orthology
1102 resource based on 5090 organisms and 2502 viruses. *Nucleic Acids Res*. 2019; doi:
1103 10.1093/nar/gky1085.
1104 104. Supek F, Bošnjak M, Škunca N, Šmuc T. REVIGO summarizes and visualizes long lists
1105 of gene ontology terms. Gibas C, editor. *PLoS ONE*. 2011; doi:
1106 10.1371/journal.pone.0021800.
1107 105. Raxworthy M. Animal cell culture: A practical approach. *Biochem Educ*. 1987; doi:
1108 10.1016/0307-4412(87)90173-7.
1109 106. Li H. Aligning sequence reads, clone sequences and assembly contigs with BWA-MEM.
1110 2013; https://arxiv.org/abs/1303.3997.
1111 107. Li H, Durbin R. Fast and accurate short read alignment with Burrows–Wheeler
1112 transform. *Bioinformatics*. 2009; doi: 10.1093/bioinformatics/btp324.
1113 108. Auwera GV der, O'Connor BD. Genomics in the cloud: using Docker, GATK, and WDL
1114 in Terra. First edition. Beijing Boston Farnham Sebastopol Tokyo: O'Reilly;
1115 109. Poplin R, Ruano-Rubio V, DePristo MA, Fennell TJ, Carneiro MO, Van Der Auwera GA,
1116 et al.. Scaling accurate genetic variant discovery to tens of thousands of samples.
1117 *Genomics.* 2017; 10.1101/201178.